Genetic causes of familial neuroblastoma

Children with either sporadic or familial NBs in connection with congenital central hypoventilation syndrome, Hirschsprung's disease, or both, usually have loss-of-function mutations in the homeobox gene *PHOX2B* [40, 41].

It was recently reported that activating mutations in the tyrosine kinase domain of the anaplastic lymphoma kinase (*ALK*) oncogene account for most cases of hereditary NB [42]. These germ-line mutations encode for single-base substitutions in key regions of the kinase domain and result in constitutive activation of the kinase and a premalignant state. Mutations resulting in oncogene activation are also somatically acquired in 5–15 % of NBs [43–45].

Thus, genetic studies of mutations in *ALK* and *PHOX2B* should be considered whenever a patient has a family history of NB or has other clinical conditions that are strongly suggestive of a highly penetrant transmissible mutation, such as bilateral primary tumors of the adrenal glands.

DNA ploidy

Hyperdiploidy (gains and losses of one or more chromosomes of a diploid genome) is a form of genetic instability frequently observed in NBs. Different patterns of hyperdiploidy seem to be associated with different clinical entities. Near-diploid and near-tetraploid NBs are usually detected in patients over 1 year of age and are related to structural abnormalities involving allelic loss of chromosome 1p/amplification of the *MYCN* gene; these features are also related to aggressive tumors and a dismal outcome. Hyperdiploid or near-triploid NBs are usually found in patients under 12 months old or in low-risk tumors (stages 1, 2, and 4s) with few or no structural chromosomal abnormalities. Near-pentaploid NBs are rare and are found in patients with favorable prognostic factors and good prognosis [46]. The mechanisms leading to this type of genetic instability in NBs are still unclear.

Cancer stem cells in NB

The heterogeneity of NB tumor histology, which suggests the existence of a self-renewing multi-potent cancer stem cell in NB, was partially addressed in the study by Ross's group. This I-type cell appears to represent a more primitive stem cell, a progenitor of N- or S-type cells, capable of both self-renewal and bidirectional differentiation. I-type cells are significantly more malignant than N- or S-type cells, with four- to five-fold greater plating efficiencies in soft agar and six-fold higher tumorigenicity in athymic mice. Furthermore, a cancer stem cell-related marker, CD133, was highly expressed in I-type, but not in N- or S-type NB cells, suggesting the role of CD133 in stem cell-like phenotypes in I-type cells [47].

Recently, Kaplan's group indicated that dissociated cells from tumors or bone marrow grew as spheres under the conditions used to culture neural crest stem cells, and these spheres were capable of self-renewal, and exhibited chromosomal aberrations typical of NB. Primary spheres from all tumor risk groups differentiated under neurogenic conditions to form neurons. Impressively, as few as 10 passaged tumor sphere cells from aggressive NB injected orthotopically into severe combined immune-deficient/Beige mice formed large NB tumors that metastasized to several organs. Furthermore, highly tumorigenic tumor spheres were isolated from the bone marrow of patients in clinical remission, suggesting that this population of cells may predict clinical behavior and serve as a biomarker for minimal residual disease in high-risk patients [48].

Kaplan and colleagues have extended their work and identified compounds that selectively target patient-derived cancer stem cell-like tumor-initiating cells (TICs) while sparing normal pediatric stem cells (skin-derived precursors, SKPs), and they have characterized two therapeutic candidates, DECA-14 and rapamycin [49].

Further, to identify the signaling pathways important for the survival and self-renewal of NB TICs and potential therapeutic targets, they screened a small molecule library of 143 protein kinase inhibitors, including 33 in clinical trials. They indicated that PLK1 may be a candidate kinase that regulates TIC growth and survival, and they found that PLK1 inhibitors seem to be promising candidates as therapy for metastatic NB [50].

CD133 (prominin-1) was the first identified member of the prominin family of cell-surface glycoproteins harboring five transmembrane domains [51]. Importantly, CD133 is a marker of TICs in many cancers [52], and therefore it may be possible to develop future therapies towards targeting cancer stem cells via this marker. A previous report indicated that "I-type" cells, which have a significantly more malignant phenotype, with 4- to 5-fold greater plating efficiency in soft agar and six-fold higher tumorigenicity in athymic mice, expressed high amounts of *CD133* miRNA compared to less malignant sub-clones [47].

To address the role of CD133 in NB tumorigenesis, we transduced *CD133* cDNA or *CD133*-knocked down shRNA by lentivirus vector in NB cell lines and primary NB tumor spheres [53]. First, we knocked down *CD133* in highly expressing NB cells and analyzed the knockdown-induced phenotype. *CD133* knockdown in highly expressing NB cells effectively resulted in significant growth retardation in adherent cell culture/soft agar culture, and a significant reduction of xenograft tumor formation in

athymic mice. In concert, ectopic CD133 expression in CD133-low NB cells accelerated proliferation and colony formation in soft agar. In *CD133* knocked-down NB cells, neurite extension and GAP43/NF68 as neuronal differentiation markers were clearly up-regulated. Expression analysis of NB cell differentiation-related growth factor receptors/ligands in CD133-expressed or -reduced NB cells indicated that RET (rearranged during transfection of the proto-oncogene) transcription was suppressed by CD133. Additionally, in 20 NB cell lines and 12 unfavorable primary NB tumors derived from patients, RET expression was markedly repressed in CD133-expressing NB cells. CD133/RET co-expression abolished the inhibition of NB cell differentiation by CD133, which was caused by CD133-related activation of the p38 mitogen-activated protein kinase (MAPK) and phosphoinositide 3 kinase (PI3K)/Akt pathways. Intriguingly, *CD133* knockdown resulted in the inhibition of tumor sphere formation in both an NB cell line and primary tumor sphere-forming cells, suggesting that CD133 appears to have a role in tumor cell stemness in NBs, which is consistent with a previous report describing that CD133+ cells showed increased sphere formation and tumorigenicity in tumor sphere-forming LAN5 NB cells [54].

CD133 was previously characterized as having five alternative promoters (P1–P5) that are active in a tissue-dependent manner [55]. The P1, P2, and P3 promoters are located within a 1540-bp CpG island, whereas promoters P4 and P5 are not encompassed by CpG-rich sequences. We intend to study the CD133-expression mechanism in NB cells, including CD133 up-regulation in sphere-forming NB cells, because we observed a positive effect of CD133 on NB tumor sphere formation. Additionally, we detected the *CD133* promoter regions mainly working in NB cells. We analyzed the important promoter regions for CD133 expression in tumor sphere-forming NB cells because a significant increase was observed in the NB tumor spheres (data not shown). An increase of CD133 at the RNA and protein levels was achieved following demethylation, as determined by assays using 5-aza-2′-deoxycytidine (5-Aza-dC) [56]. The significance of CD133 promoter methylation in tumorigenesis in several tumors is still unresolved [57, 58].

Acknowledgments We thank Mr. Daniel Mrozek, Medical English Service, for editorial assistance. This work was supported in part by a Grant-in-Aid from the National Cancer Center Research and Development Fund of Japan (4), a Grant-in-Aid from the Ministry of Health, Labor, and Welfare of Japan for Third Term Comprehensive Control Research for Cancer, a Grant-in-Aid for Scientific Research (B) (24390269), and a Grant-in-Aid from the Uehara Memorial Foundation.

Conflict of interest We have no financial relationships to disclose.

References

1. Westermann F, Schwab M (2002) Genetic parameters of neuroblastomas. Cancer Lett 184:127–147
2. Maris JM, Hogarty MD, Bagatell R et al (2007) Neuroblastoma. Lancet 369:2106–2120
3. van Noesela MM, Versteeg R (2004) Pediatric neuroblastomas: genetic and epigenetic 'danse macabre'. Gene 325:1–15
4. D'Angio GJ, Evans AE, Koop CE (1971) Special pattern of widespread neuroblastoma with a favourable prognosis. Lancet 297:1046–1049
5. Kato GJ, Lee WM, Chen LL et al (1992) Max: functional domains and interaction with c-Myc. Genes Dev 6:81–92
6. Zindy F, Eischen CM, Randle DH et al (1998) Myc signaling via the ARF tumor suppressor regulates p53-dependent apoptosis and immortalization. Genes Dev 12:2424–2433
7. Kohl NE, Kanda N, Schreck RR et al (1983) Transposition and amplification of oncogene related sequence in human neuroblastomas. Cell 35:359–367
8. Schwab M, Alitalo K, Klempnauer KH et al (1983) Amplified DNA with limited homology to myc cellular oncogene is shared by human neuroblastoma cell lines and a neuroblastoma tumor. Nature 305:245–248
9. Corvi R, Amler LC, Savelyeva L et al (1994) MYCN is retained in single copy at chromosome 2 band p23–24 during amplification in human neuroblastoma cells. Proc Natl Acad Sci USA 91:5523–5527
10. Schwab M (1998) Amplification of oncogenes in human cancer cells. Bioessays 20:473–479
11. Seeger RC, Brodeur GM, Sather H et al (1985) Association of multiple copies of the N-myc oncogene with rapid progression of neuroblastomas. N Engl J Med 313:1111–1116
12. Brodeur G, Seeger RC, Schwab M et al (1984) Amplification of N-myc in untreated human neuroblastomas correlates with advanced disease stage. Science 224:1121–1124
13. Rubie H, Hartmann O, Michon J et al (1997) Localized neuroblastoma: MYCN amplification is the main prognostic factor-results of the NBL 90 study. J Clin Oncol 15:1171–1182
14. Caron H (1995) Allelic loss of chromosome 1 and additional chromosome 17 material are both unfavourable prognostic markers in neuroblastoma. Med Pediatr Oncol 24:215–221
15. Bown N, Cotterill S, Lastowska M et al (1999) Gain of chromosome arm 17q and adverse outcome in patients with neuroblastoma. N Engl J Med 340:1954–1961
16. Okabe-Kado J, Kasukabe T, Honma Y et al (2005) Clinical significance of serum NM23-H1 protein in neuroblastoma. Cancer Sci 96:653–660
17. Adida C, Berrebi D, Peuchmaur M et al (1998) Anti-apoptosis gene, survivin, and prognosis of neuroblastoma. Lancet 351:882–883
18. White PS, Maris JM, Beltinger C et al (1995) A region of consistent deletion in neuroblastoma maps within 1p36.2-3. Proc Natl Acad Sci USA 92:5520–5524
19. Caron H, Spieker N, Godfried M et al (2001) Chromosome bands 1p35–36 contain two distinct neuroblastoma tumor suppressor loci, one of which is imprinted. Genes Chromosom Cancer 30:168–174
20. Bauer A, Savelyeva L, Claas A et al (2001) Smallest region of overlapping deletion in 1p36 in human neuroblastoma: a 1 Mbp cosmid and PAC contig. Genes Chromosom Cancer 31:228–239
21. Brodeur GM (2003) Neuroblastoma: biological insights into a clinical enigma. Nat Rev Cancer 3:203–216
22. Wei JS, Song YK, Durinck S et al (2008) The MYCN oncogene is a direct target of miR-34a. Oncogene 27:5204–5213

23. Cole KA, Attiyeh EF, Mosse YP et al (2008) A functional screen identifies miR-34a as a candidate neuroblastoma tumor suppressor gene. Mol Cancer Res 6:735–742
24. Bagchi A, Papazoglu C, Wu Y et al (2007) CHD5 is a tumor suppressor at human 1p36. Cell 128:459–475
25. Munirajan AK, Ando K, Mukai A et al (2008) KIF1Bbeta functions as a haploinsufficient tumor suppressor gene mapped to chromosome 1p36.2 by inducing apoptotic cell death. J Biol Chem 283:24426–24434
26. Guo C, White PS, Weiss MJ et al (1999) Allelic deletion at 11q23 is common in MYCN single copy neuroblastomas. Oncogene 18:4948–4957
27. Spitz R, Hero B, Ernestus K et al (2003) Deletions in chromosome arms 3p and 11q are new prognostic markers in localized and 4s neuroblastoma. Clin Cancer Res 9:52–58
28. Attiyeh EF, London WB, Mosse YP et al (2005) Chromosome 1p and 11q deletions and outcome in neuroblastoma. N Engl J Med 353:2243–2253
29. Cohn SL, Pearson AD, London WB et al (2009) The International Neuroblastoma Risk Group (INRG) classification system: an INRG Task Force report. J Clin Oncol 27:289–297
30. Tomioka N, Oba S, Ohira M et al (2008) Novel risk stratification of patients with neuroblastoma by genomic signature which is independent of molecular signature. Oncogene 27:441–449
31. Ando K, Ohira M, Ozaki T et al (2008) Expression of TSLC1, a candidate tumor suppressor gene mapped to chromosome 11q23, is downregulated in unfavorable neuroblastoma without promoter hypermethylation. Int J Cancer 123:2087–2094
32. Ochiai H, Takenobu H, Nakagawa A et al (2010) Bmi1 is a MYCN target gene and regulates tumorigenesis via repression of KIF1Bβ and TSLC1 in neuroblastoma. Oncogene 29:2681–2690
33. Kogner P, Barbany G, Dominici C et al (1993) Coexpression of messenger RNA for TRK protooncogene and low affinity nerve growth factor receptor in neuroblastoma with favorable prognosis. Cancer Res 53:2044–2050
34. Nakagawara A, Arima-Nakagawara M, Scavarda NJ et al (1993) Association between high levels of expression of the TRK gene and favorable outcome in human neuroblastoma. N Engl J Med 328:847–854
35. Nakagawara A, Azar CG, Scavarda NJ et al (1994) Expression and function of TRK-B and BDNF in human neuroblastomas. Mol Cell Biol 14:759–767
36. Eggert A, Grotzer MA, Zuzak TJ et al (2001) Resistance to tumor necrosis factor-related apoptosis-inducing ligand (TRAIL)-induced apoptosis in neuroblastoma cells correlates with a loss of caspase-8 expression. Cancer Res 61:1314–1319
37. Teitz T, Wei T, Valentine MB et al (2000) Caspase 8 is deleted or silenced preferentially in childhood neuroblastomas with amplification of MYCN. Nat Med 6:529–535
38. Ejeskar K, Aburatani H, Abrahamsson J et al (1998) Loss of heterozygosity of 3p markers in neuroblastoma tumours implicate a tumour-suppressor locus distal to the FHIT gene. Br J Cancer 77:1787–1791
39. Astuti D, Agathanggelou A, Honorio S et al (2001) RASSF1A promoter region CpG island hypermethylation in phaeochromocytomas and neuroblastoma tumours. Oncogene 20:7573–7577
40. Mosse YP, Laudenslager M, Khazi D et al (2004) Germline PHOX2B mutation in hereditary neuroblastoma. Am J Hum Genet 75:727–730
41. Trochet D, Bourdeaut F, Janoueix-Lerosey I et al (2004) Germline mutations of the paired-like homeobox 2B (PHOX2B) gene in neuroblastoma. Am J Hum Genet 74:761–764
42. Mossé YP, Laudenslager M, Longo L et al (2008) Identification of ALK as a major familial neuroblastoma predisposition gene. Nature 455:930–935
43. Janoueix-Lerosey I, Lequin D, Brugières L et al (2008) Somatic and germline activating mutations of the ALK kinase receptor in neuroblastoma. Nature 455:967–970
44. George RE, Sanda T, Hanna M et al (2008) Activating mutations in ALK provide a therapeutic target in neuroblastoma. Nature 455:975–978
45. Chen Y, Takita J, Choi YL et al (2008) Oncogenic mutations of ALK kinase in neuroblastoma. Nature 455:971–974
46. Look AT, Hayes FA, Shuster JJ et al (1991) Clinical relevance of tumor cell ploidy and N-myc gene amplification in childhood neuroblastoma: a Pediatric Oncology Group study. J Clin Oncol 9:581–591
47. Walton JD, Kattan DR, Thomas SK et al (2004) Characteristics of stem cells from human neuroblastoma cell lines and in tumors. Neoplasia 6:645–838
48. Hansford LM, McKee AE, Zhang L et al (2007) Neuroblastoma cells isolated from bone marrow metastases contain a naturally enriched tumor-initiating cell. Cancer Res 67:11234–11243
49. Smith KM, Datti A, Fujitani M et al (2010) Selective targeting of neuroblastoma tumour-initiating cells by compounds identified in stem cell-based small molecule screens. EMBO Mol Med 2:371–384
50. Grinshtein N, Datti A, Fujitani M et al (2011) Small molecule kinase inhibitor screen identifies polo-like kinase 1 as a target for neuroblastoma tumor-initiating cells. Cancer Res 71:1385–1395
51. Corbeil D, Fargeas CA, Huttner WB (2001) Rat prominin, like its mouse and human orthologues, is a pentaspan membrane glycoprotein. Biochem Biophys Res Commun 285:939–944
52. O'Brien CA, Kreso A, Jamieson CHM (2010) Cancer stem cells and self-renewal. Clin Cancer Res 16:3113–3120
53. Takenobu H, Shimozato O, Nakamura T et al (2011) CD133 suppresses neuroblastoma cell differentiation via signal pathway modification. Oncogene 30:97–105
54. Mahller YY, Williams JP, Baird WH et al (2009) Neuroblastoma cell lines contain pluripotent tumor initiating cells that are susceptible to a targeted oncolytic virus. PLoS ONE 4:e4235
55. Shmelkov SV, Jun L, St Clair R et al (2004) Alternative promoters regulate transcription of the gene that encodes stem cell surface protein AC133. Blood 103:2055–2061
56. Schiapparelli P, Enguita-Germán M, Balbuena J et al (2010) Analysis of stemness gene expression and CD133 abnormal methylation in neuroblastoma cell lines. Oncol Rep 24:1355–1362
57. Baba T, Convery PA, Matsumura N et al (2009) Epigenetic regulation of CD133 and tumorigenicity of CD133+ ovarian cancer cells. Oncogene 28:209–218
58. Yi JM, Tsai HC, Glöckner SC et al (2008) Abnormal DNA methylation of CD133 in colorectal and glioblastoma tumors. Cancer Res 68:8094–8103

Published OnlineFirst July 19, 2012; DOI:10.1158/0008-5472.CAN-12-0943

Cancer Research

NLRR1 Enhances EGF-Mediated *MYCN* Induction in Neuroblastoma and Accelerates Tumor Growth *In Vivo*

Shamim Hossain, Atsushi Takatori, Yohko Nakamura, et al.

Cancer Res 2012;72:4587-4596. Published OnlineFirst July 19, 2012.

Published OnlineFirst July 19, 2012; DOI:10.1158/0008-5472.CAN-12-0943

Cancer Research

NLRR1 Enhances EGF-Mediated *MYCN* Induction in Neuroblastoma and Accelerates Tumor Growth *In Vivo*

Shamim Hossain[1], Atsushi Takatori[1], Yohko Nakamura[1], Yusuke Suenaga[1], Takehiko Kamijo[2], and Akira Nakagawara[1]

Abstract

Neuronal leucine-rich repeat protein-1 (NLRR1), a type-1 transmembrane protein highly expressed in unfavorable neuroblastoma, is a target gene of MYCN that is predominately expressed in primary neuroblastomas with *MYCN* amplification. However, the precise biological role of NLRR1 in cell proliferation and tumor progression remains unknown. To investigate its functional importance, we examined the role of NLRR1 in EGF and insulin growth factor-1 (IGF-1)–mediated cell viability. We found that NLRR1 positively regulated cell proliferation through activation of extracellular signal–regulated kinase mediated by EGF and IGF-1. Interestingly, EGF stimulation induced endogenous *MYCN* expression through Sp1 recruitment to the *MYCN* promoter region, which was accelerated in NLRR1-expressing cells. The Sp1-binding site was identified on the promoter region for *MYCN* induction, and phosphorylation of Sp1 was important for EGF-mediated MYCN regulation. *In vivo* studies confirmed the proliferation-promoting activity of NLRR1 and established an association between *NLRR1* expression and poor prognosis in neuroblastoma. Together, our findings indicate that NLRR1 plays an important role in the development of neuroblastoma and therefore may represent an attractive therapeutic target for cancer treatment. *Cancer Res; 72(17); 4587–96. ©2012 AACR.*

Introduction

Neuroblastoma is one of the most common extracranial malignant tumors that develop in children; they arise from neural crest cells and are mostly found in the adrenal medulla or along the sympathetic chain (1). neuroblastoma exhibits clinical and biological heterogeneity, ranging from rapid progression associated with metastatic spread and poor clinical outcome to occasional, spontaneous, or therapy-induced regression or differentiation into benign ganglioneuroma (2, 3). Different subsets of neuroblastoma show various distinct genetic features, including DNA ploidy, *MYCN* amplification, allelic loss of the distal part of chromosome 1p, and gain of chromosome 17q (4). Amplification of the *MYCN* gene usually distinguishes a subset of neuroblastoma with poor prognosis (1), and recovery of children with high-risk neuroblastoma remains low, providing a compelling reason for better understanding of the molecular mechanisms that can be targeted to treat this disease (5, 6). *MYCN* transgenic mice develop neuroblastoma, which implicates that MYCN can maintain the tumorigenic state, supporting the importance of the *MYCN* gene as a potential therapeutic target (7–9). However, the precise mechanism of *MYCN* regulation and the functional correlation with other proteins in the progression of neuroblastoma are still elusive.

NLRR1 is a type I transmembrane protein with extracellular leucine-rich repeats, and belongs to the mammalian neuronal leucine-rich protein family (NLRR1–NLRR5; ref. 10–13). We previously reported that mRNA expression levels of *NLRR1* are significantly higher in unfavorable neuroblastoma (12). We further reported that NLRR1 protein expression is higher in *MYCN*-amplified primary neuroblastomas than in nonamplified tumors, and that MYCN can transcriptionally upregulate *NLRR1* (14). We also found that overexpression of NLRR1 promoted neuroblastoma cell proliferation and inhibited cellular apoptosis upon serum starvation (14). NLRR family proteins have also been considered as cell adhesion or signaling molecules, and mouse NLRR3 functions in EGF-mediated activation of extracellular signal–regulated kinase (ERK; ref. 15).

EGF signaling was reported to be involved in neuroblastoma cell proliferation via the activation of ERK and AKT (16). Insulin growth factor-I (IGF-I) stimulation was also reported to enhance neuroblastoma cell proliferation, and is involved in the induction of *MYCN* expression through mitogen-activated protein kinase (MAPK; ref. 17). MAPK kinase (MKK) proteins are crucially important in several cellular events, including proliferation, survival, and differentiation (18, 19). Several stimuli activate MKKs, which is followed by activation of MAPKs, including ERK, JNK, and p38 MAPK. Abnormalities in MAPK pathways, especially mutations of proteins of these signaling cascades, have been reported in about 20% of all

Authors' Affiliations: Divisions of [1]Biochemistry & Innovative Cancer Therapeutics and [2]Biochemistry and Molecular Carcinogenesis, Chiba Cancer Center Research Institute, Chiba, Japan

Note: Supplementary data for this article are available at Cancer Research Online (http://cancerres.aacrjournals.org/)

Corresponding Author: Akira Nakagawara, Division of Biochemistry & Innovative Cancer Therapy, Chiba Cancer Center Research Institute, 666-2 Nitona, Chuoh-ku, Chiba 260-8717, Japan. Phone: 81-43-264-5431; Fax: 81-43-265-4459; E-mail: akiranak@chiba-cc.jp

doi: 10.1158/0008-5472.CAN-12-0943

Published OnlineFirst July 19, 2012; DOI:10.1158/0008-5472.CAN-12-0943

human cancers (20, 21). Several reports suggest that MKK/ERK signaling has an important role in tumorigenesis and metastasis (22–24). However, the precise role of MKK/ERK signaling in the development of neuroblastoma and its functional relationship with *MYCN* oncogene are still unknown. NLRR1 is a possible regulator of growth factor signaling, and may play a crucial role in *MYCN*-amplified neuroblastoma to form aggressive tumors. In this study, we report that EGF promotes ERK activation and is involved in *MYCN* induction via recruitment of Sp1 to the *MYCN* promoter. Overexpression of NLRR1 enhanced *MYCN* induction by activating ERK signaling, whereas knockdown of *NLRR1* suppressed ERK phosphorylation and *MYCN* induction upon EGF treatment. *In vivo* studies in nude mice showed significant tumorigenic activity of NLRR1. Our present findings collectively indicate that NLRR1 accelerates growth factor signaling to induce *MYCN*, and plays a positive feedback loop with MYCN to induce aggressive tumor progression in neuroblastoma.

Materials and Methods

Cell lines, transfection, and reagents

Human neuroblastoma-derived SK-N-BE and SH-SY5Y cells were collected from CHOP cell lines and were maintained in RPMI 1640 medium supplemented with 10% heat-inactivated fetal bovine serum (Invitrogen), 50 μg/mL penicillin, and 50 μg/mL streptomycin (Invitrogen). Cells were cultured in a humidified atmosphere of 5% CO^2 and 95% air at 37°C. For transient transfection, SK-N-BE cells were transfected with the indicated plasmids using Lipofectamine 2000 (Invitrogen) according to the manufacturer's instructions.

Cell proliferation assays

SK-N-BE and SH-SY5Y cell proliferation was evaluated using the tetrazolium compound WST-8 (Cell Counting Kit-8 Dojindo Laboratories, Japan). Cell proliferation was determined according to the manufacturer's instructions.

RNA extraction and reverse transcription-PCR

Total RNA was prepared from the indicated cells using the RNeasy Mini Kit (Qiagen) according to the manufacturer's protocol, and reverse-transcription was performed. The specific primers used were as follows: *MYCN*, 5′-CTTCGGTCCAGCTTTCTCAC-3′ and 5′-GTCCGAGCGTGTTCAATTTT-3′; NLRR1, 5-GCAGCTTTTCAACTTGACTGAA-3 and 5-TGCAGCAGCTTTTCAACTTGACTGAAC-3; *VEGF*, 5′-AAGGAGGAGGGCAGAATCAT-3′ and 5′-ATCTGCATGGTGATGTTGGA-3′; *Sp1*, 5′-TGCAGCAGAATTGAGTCACC -3′ and 5′- CACAACATACTGCCCACCAG-3′; *GAPDH*, 5′- ACCTGACCTGCCGTCTAGAA-3′ and 5′-TCCACCACCCTGTTGCTGTA-3′. *GAPDH* expression was measured as an internal control.

Immunoblotting

Cells were collected and washed with PBS. Whole cell lysates were prepared by incubating cells in lysis buffer containing 10 mmol/L Tris-HCl, pH 8.0, 150 mmol/L NaCl, 2 mmol/L ethyleneglycol tetraacetic acid, 50 mmol/L β-mercaptoethanol, 1% Triton X-100, a commercial protease inhibitor mixture (Sigma), and phosphatase inhibitor mixture (Sigma), for 30 minutes on ice, and subjected to brief sonication for 10 seconds at 4°C, followed by centrifugation at 15,000 rpm at 4°C for 10 minutes to remove insoluble materials. Protein concentration was measured using the BCA Protein Assay Kit (Thermo Scientific) according to the manufacturer's instruction. Equal amounts of protein (50 μg) were separated by 7.5% SDS-PAGE and electrophoretically transferred onto polyvinylidene difluoride (PVDF) membranes (Immobilion-P, Millipore. PVDF membranes were then blocked with TBS containing 5% nonfat dry milk and 0.1% Tween 20 at room temperature for 1 hour. After blocking, the membranes were incubated at 4°C overnight with anti-MYCN (Ab-1, Oncogene), anti-EGFR (Rockland), anti-actin (20–33; Sigma), and other antibodies against ERK1/2, phospho-ERK, IGF1R, phospho IGFR1, Akt, phospho-Akt, and phospho-EGFR were purchased from Cell Signaling Technology. After incubation with primary antibodies, membranes were incubated with horseradish peroxidase-coupled goat anti-mouse or anti-rabbit IgG secondary antibody (Cell Signaling Technology) for 1 hour at room temperature. Immunoblots were visualized using ECL detection reagents according to the manufacturer's instruction (Amersham Biosciences).

Construction of luciferase reporters

A luciferase reporter construct driven by the *MYCN* promoter was generated by using the following primer sets: MYCN (−221/+21), 5′- GAGCTCCAGCTTTGCAGCCTTCTC-3′ and 5′- GAGCTCGTCCAGACAGATGACTGTC-3′. Underlined sequences indicate *SacI* enzyme recognition sites. Then, the PCR product was inserted into the *SacI* site of pGL3 basic vector. Mutation of the 2 putative Sp1-binding sites was performed using a site-directed mutagenesis kit (Promega) using the following primer sets: mut-1 (−221/+21), 5′-ACAGCCCCCTTCTCTCCCC(A)G(A)CCC(A)CCCGG-3′(sense), 5′-GGGAGAGAAGGGGGCTGTGGCGCA-3′ (antisense); mut-2 (−221/+21), 5′-ATGGAAATCAGGAGGGC(A)G(A)GGGTAAAG-3′(sense), 5′-CCCTCCTGATTTCCATAAAAATCA-3′ (antisense). Underlined sequences represent putative Sp1-binding sites, and the mutated nucleotides are marked by brackets.

Luciferase reporter assays

SK-N-BE cells were plated in 12-well plates at a density of 50,000 cells/well, and transiently transfected with reporter constructs driven by the *MYCN* promoter (200 ng) and pRL-TK *Renilla* luciferase reporter plasmid (20 ng). After the indicated time periods, cells were collected and washed with PBS, and their luciferase activities were measured using a luciferase reporter assay system (Promega). Each experiment was performed at least 3 times in triplicate.

siRNA transfection

A mixture of 2 siRNAs with antisense sequences of 5′-UCUUGGUUGAGCUGUGUAGTT-3′ and 5′-UUGUGGACACUCACUAUUCTT-3′ were designed to target human *NLRR1* (TAKARA). Control siRNA was purchased from Ambion (Cat 4635). SK-N-BE cells were transfected with 20 nmol/L of the indicated siRNAs using Lipofectamine RNAiMAX (Invitrogen).

Published OnlineFirst July 19, 2012; DOI:10.1158/0008-5472.CAN-12-0943

ChIP assays

Before collection, cells were cross-linked with 1% formaldehyde in medium for 10 minutes at 37°C. Chromatin immunoprecipitation (ChIP) was performed following the protocol provided by Upstate Biotechnology. In short, cross-linked chromatin was prepared from cells and sonicated to an average length of 200 to 800 nucleotides, precleaned with protein A-agarose beads pretreated with shared salmon sperm DNA, and immunoprecipitated with rabbit anti-E2F1 (KH95, Santa Cruz) and rabbit anti-Sp1 (DAM1718081, Upstate/Millipore) antibodies conjugated with protein A-agarose. The immunoprecipitates were eluted with 100 μL elution buffer (1% SDS and 0.1 mol/L $NaHCO_3$). Formaldehyde-mediated cross-links were reversed by heating at 65°C for 4 hours, and the reaction mixtures were treated with proteinase K at 45°C for 1 hour. Precipitated DNA and control input DNA were purified using a QIAquick PCR Purification Kit (Qiagen). Purified DNA was amplified by PCR using the following primer set: 5′- CAGCTTTGCAGCCTTCTC-3′ and 5′-GTCCAGACAGATGACTGTC-3′ targeting the MYCN core promoter region (−221, +21).

Animals and tumor xenograft studies

Male BALB/c athymic (nu/nu) mice (5–6 weeks old) were purchased from Japan SLC, and maintained under specific pathogen-free conditions strictly following the Chiba Cancer Center Research Institute guidelines. Stably expressing NLRR1 and mock SH-SY5Y cell lines were established by transfection followed by selection with G418 at a concentration of 600 μg/mL for about 6 to 8 weeks. Single colonies were picked to confirm the ectopic expression of NLRR1. Three NLRR1-expressing clones were used for the tumor xenograft studies, and 3 mock-transfected single clones were used as negative controls. A total of 6 groups of mice (7 mice in each group) received subcutaneous injections of 1×10^7 cells dissolved in 100 μL PBS. The length and width of each tumor was recorded each week at the indicated time periods. Tumor volume was calculated according the following formula: [length × $(\text{width})^2$]/2 (25, 26). Survival curves were generated using the Kaplan–Meier method using SPSS software. Log-rank tests were performed to calculate the *P* value between the 2 survival curves.

Immunohistochemical staining

To prepare the cryosections, tumors were fixed in 4% paraformaldehyde, washed with sucrose solution, embedded in OCT compound, frozen, and sectioned at 10 μm thickness. Sections were air-dried, washed with TBS, blocked in Mouse on Mouse blocking solution (MOM; PK-2200, Vector Laboratories) with 5% goat serum and 2% bovine serum albumin, and then treated with MOM diluent. Sections were then incubated with anti-NLRR1 (TB776, affinity purified, MBL) and anti-Ki-67 (mouse monoclonal 556003, BD) antibodies. MOM anti-mouse IgG and rabbit Alexa 488 were used as secondary antibodies followed by Fluorescein Avidin CY3 (Vector Laboratories). DAPI was used to stain the nuclei.

Four-mm thick paraffin tissue sections of the mock and NLRR1 tumors were subjected to immunohistochemistry (IHC). After deparafinization antigen retrieval was performed by boiling with 0.1 mol/L citrate buffer (pH 6.0) using microwave at 800 W for 10 minutes. The primary antibody for NMYC (Ab-1, Oncogene), p-ERK (4376, Cell signaling), and ERK (4695, Cell signaling) was used at1:100 dilutions followed by the

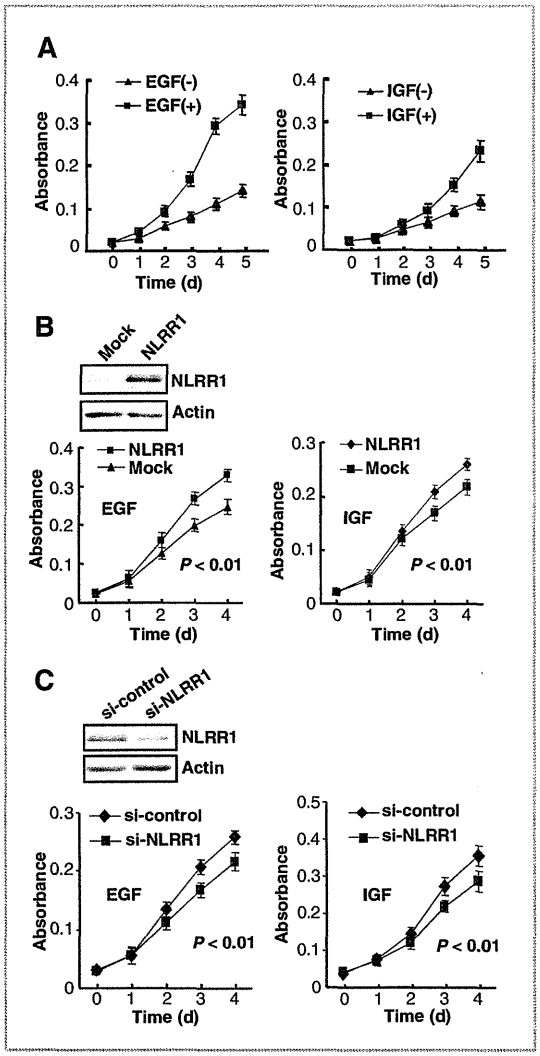

Figure 1. NLRR1 promotes EGF/IGF-mediated cell proliferation. A, quantification of SK-N-BE cell proliferation following EGF (left) and IGF (right) stimulation for the indicated time periods using WST-8 assays. The data are represented as mean ± SD. B, ectopic expression of NLRR1 in SK-N-BE cells was confirmed by immunoblotting (top). NLRR1-expressing SK-N-BE cells were treated with EGF (left) and IGF (right) for the indicated time periods, and proliferation was measured by WST-8 assays. C, NLRR1 knockdown by transfection with siRNA was confirmed by immunoblotting (top). Growth curve of SK-N-BE cells transfected with control siRNA and siRNA against NLRR1 in the presence of EGF (left) and IGF (right) was measured by WST-8 assays. For all WST-8 assays (A, B, and C), cells were cultured in 2% serum-containing medium, and growth factors were used at a concentration of 50 ng/mL.

Published OnlineFirst July 19, 2012; DOI:10.1158/0008-5472.CAN-12-0943

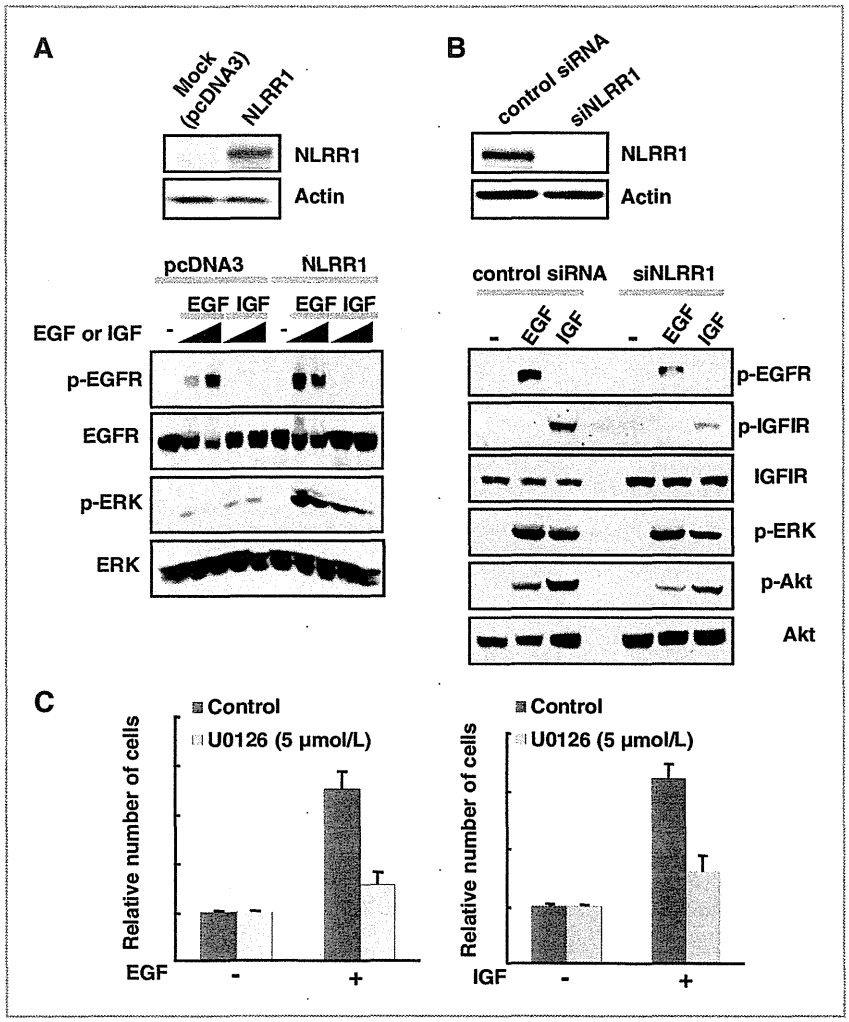

Figure 2. NLRR1 enhances EGF and IGF-mediated phosphorylation of ERK. A, SK-N-BE cells were transiently transfected with mock (pCDNA3) and NLRR1-expressing plasmid. Forty-eight hours after transfection, cells were starved with serum-free medium for 12 hours and then stimulated with EGF and IGF for 10 minutes. Whole cell lysates were used for immunoblotting with specific antibodies (bottom). NLRR1 overexpression was confirmed by immunoblotting of the same lysates (top). B, siRNA-mediated knockdown of NLRR1 suppresses phosphorylation of ERK mediated by EGF and IGF (bottom). The experimental conditions are similar to those in A. Knockdown efficiency was confirmed by immunoblotting (top). C, SK-N-BE cells transfected with NLRR1-expressing plasmids were pretreated with MEK1/2-specific inhibitor (U0126) and then cultured in the presence or absence of EGF and IGF; cell proliferation was measured by WST-8 assays.

standard protocol of Cell signaling. Secondary biotinylated universal antibody from Vector Laboratories was applied at a dilution of 1:400. Reactivity was visualized with an avidin-biotin complex immunoperoxidase system using diaminobenzidine as the chromagen and Hematoxylin as the counterstain (Vector Laboratories).

Results

NLRR1 enhances EGF/IGF-mediated cell proliferation in neuroblastoma cells

Our previous report showed that *NLRR1* is a direct transcriptional target of MYCN in neuroblastoma, and is associated with cell proliferation and survival (14). However, the mechanism by which NLRR1 regulates cell proliferation was still unknown. Another member of leucine rich repeat protein family, NLRR3, has been associated with the activation of ERK (15), and EGFR activation was reported to accelerate neuroblastoma cell proliferation (16), suggesting the possibility that NLRR1 may activate EGFR to induce cell proliferation. To test this hypothesis, we first investigated neuroblastoma cell proliferation upon EGF and IGF-I treatment. Consistent with their proliferative role (16, 17), both EGF and IGF-I also accelerated the proliferation of SK-N-BE cells (Fig. 1A). Similar data were also observed in neuroblastoma SH-SY5Y cells (data not shown). To determine whether NLRR1 promotes EGF- and IGF-1–mediated cell proliferation, we transiently transfected SK-N-BE cells with NLRR1 expression plasmid and treated them with EGF and IGF-I. Interestingly, ectopic expression of NLRR1 enhanced the cell proliferation mediated by EGF and IGF-I (Fig. 1B). Overexpression of NLRR1 in SH-SY5Y showed similar promotion of proliferation (data not shown). To confirm the role of NLRR1, we used an RNA interference approach to knock down endogenous *NLRR1*. The data suggested that knockdown of *NLRR1* suppressed the EGF- and IGF-1–mediated cell proliferation (Fig. 1C). Collectively, the data suggested

Published OnlineFirst July 19, 2012; DOI:10.1158/0008-5472.CAN-12-0943

that NLRR1 enhances cell proliferation mediated by EGF and IGF-I.

NLRR1 enhances EGF and IGF-mediated activation of ERK

Because ERK is an important kinase that is often regulated by EGF and IGF-1 growth factors to induce cell proliferation, we were interested to determine whether NLRR1 affected ERK phosphorylation upon EGF and IGF-I treatment. We examined the activation of ERK in NLRR1-overexpressing cells. Interestingly, ERK phosphorylation was enhanced compared with the mock-transfected cells (Fig. 2A). The increased phosphorylation of EGFR was observed in the NLRR1 overexpressing SK-N-BE cells upon EGF stimulation (Fig. 2A). Similar data were also observed in SH-SY5Y cells (data not shown). We also used siRNA studies to further elucidate the role of NLRR1 in EGF and IGF-1 signaling. Consistent with the overexpression study, we observed a reduction in ERK phosphorylation in *NLRR1* knockdown cells upon both EGF and IGF-1 treatment compared with the control siRNA-transfected cells (Fig. 2B). Interestingly, phosphorylation of EGFR and IGFR was found to be decreased in NLRR1 knockdown cells (Fig. 2B). To elucidate whether the activation of ERK is important for cell proliferation, we used the MEK1/2-specific inhibitor, U0126 (27), in the cell proliferation assays. For the cell proliferation assays, we have used the minimum concentration of U0126 (5 μmol/L) required to inhibit ERK activation in the cells (Supplementary Fig. S1). The data showed that EGF- and IGF-I–mediated proliferation of NLRR1-overexpressing SK-N-BE cells was inhibited upon U0126 treatment (Fig. 2C).

EGF stimulation induces *MYCN* via ERK

IGF-I stimulation induces endogenous *MYCN* expression in neuroblastoma cells via MAPK activation (17). Therefore, it is possible that EGF can induce *MYCN*, because EGF treatment also activates MAPK. To investigate this hypothesis, we treated SK-N-BE cells cultured in serum-free medium with increasing amounts of EGF. Consistent with our hypothesis, both mRNA and protein levels of MYCN were induced upon EGF treatment (Fig. 3A). Time course experiments were also used to confirm that EGF can induce *MYCN*. *MYCN* was found to be induced at 6 hours after EGF treatment (Fig. 3B). Under our experimental conditions, EGF treatment successfully phosphorylated EGFR (Supplementary Fig. S1) and ERK (data not shown). We also observed that EGF stimulation induced *MYCN* expression in other neuroblastoma cell lines, SH-SY5Y and NLF (data not shown). To verify our experimental data that EGF induces *MYCN*, we used *VEGF* as positive control, which was reported to be induced by EGF (28). AG1478 is a specific inhibitor for EGFR, and is sufficient to block EGFR-mediated activation of ERK (29, 30). We have confirmed the effect of the optimum concentration of AG1478 to inhibit EGF-mediated phosphorylation of EGFR in the cells (Supplementary Fig. S1). Therefore, we used the optimum concentrations of AG1478 to elucidate that EGF-mediated *MYCN* induction is dependent on EGFR-ERK signaling. Consistently, *MYCN* induction by EGF was successfully blocked in AG1478-pretreated SK-N-BE cells (Fig. 3C left). We also used U0126 to prove that EGF-mediated *MYCN* induction is dependent on ERK (Fig. 3C, right panel). These data collectively suggest that EGF-mediated *MYCN* induction is dependent on the EGFR–ERK pathway in neuroblastoma cells.

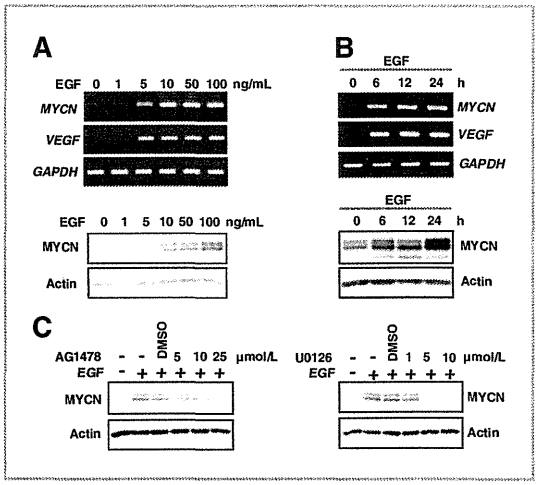

Figure 3. EGF stimulation induces endogenous *MYCN*. A, serum-starved SK-N-BE cells were treated with increasing doses of EGF for 12 hours. Total mRNA was used in reverse transcription (RT)-PCR to check the expression of *MYCN* and *VEGF* (top). *GAPDH* was checked as an internal control. Whole cell lysates were used in immunoblotting to detect the proteins (bottom). B, MYCN was induced by EGF in a time-dependent manner. Serum-starved SK-N-BE cells were treated with 50 ng/mL of EGF. Total RNA and whole cell lysates were collected at the indicated time points for RT-PCR (top) and Western blotting (bottom) assays to check the expression level of MYCN. C, SK-N-BE cells were cultured in serum-free medium for 12 hours with or without different concentrations of AG1478 (left) and U0126 (right). Cells were then treated with EGF (50 ng/mL) for 12 hours, and whole cell lysates were used to check MYCN protein levels by immunoblotting. Actin was checked as an internal control.

EGF enhances *MYCN* transcription via recruitment of Sp1 to the *MYCN* promoter

To confirm the EGF-mediated *MYCN* transcription, we generated a luciferase reporter plasmid containing a *MYCN* genomic fragment spanning positions −221 to +21 (Fig. 4A, left panel), where +1 represents the transcriptional initiation site. This promoter region contains both Sp1 and E2F1 transcriptional element sites (31, 32). We also used the empty control vector pGL3basic to compare the EGF responses. SK-N-BE cells were transiently transfected with pGL3basic and pGL3-*MYCN* (−221, +21) together with *Renilla* luciferase reporter plasmid. The data showed that EGF stimulation significantly enhanced the promoter activity of *MYCN* gene at 6 hours (Fig. 4A, right panel): pGL3-Basic reporter constructs did not respond to EGF treatment (Fig. 4A, right), suggesting that EGF treatment is specific to the *MYCN* promoter. *MYCN* has been reported to be transcriptionally regulated by 2 major transcription factors, Sp1 and E2F1 (31, 32). To determine the regulatory mechanism of EGF-mediated *MYCN* transcription, we performed ChIP assays. Both antibodies against Sp1 and E2F1 used for ChIP assays pulled down the specific

Published OnlineFirst July 19, 2012; DOI:10.1158/0008-5472.CAN-12-0943

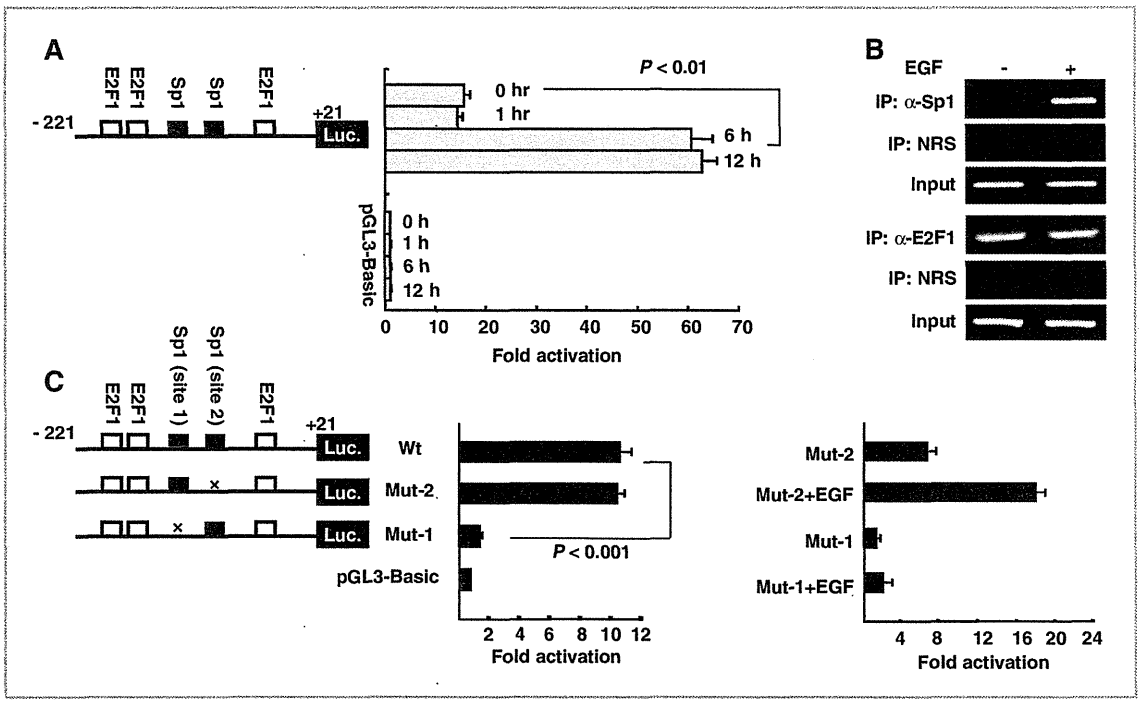

Figure 4. EGF enhances Sp1-mediated transactivation of *MYCN*. A, *MYCN* core promoter region (−221 to +21) cloned in pGL3Basic luciferase vector (left) was transiently transfected into SK-N-BE cells for 36 hours, followed by culture in serum-free medium for 12 hours. Cells were then treated with EGF (50 ng/mL) for the indicated time periods, and luciferase assays were carried out to quantify the relative promoter activity. B, SK-N-BE cells were cultured in serum-free medium for 12 hours, followed by treatment for 12 hours with EGF (50 ng/mL). Cross-linked chromatin was isolated from the cells and precipitated with Sp1- and E2F1-specific antibodies or with normal rabbit serum (NRS). C, Sp1 site 1-deleted *MYCN* core promoter failed to respond to EGF stimulation. Two Sp1-binding sites on the *MYCN* core promoter region were deleted by site-directed mutagenesis (left). Relative activity of the deleted promoter constructs were measured by luciferase assays in SK-N-BE cells 24 hours after transfection (middle). SK-N-BE cells were transiently transfected by the 2 Sp1 site deleted constructs, followed by culture in serum-free medium for 12 hours and then treatment with EGF (50 ng/mL). Twelve hours after EGF treatment, firefly luciferase activities were determined (right). *Renilla* luciferase was used as an internal control to standardize the transfection efficiency of the luciferase vectors.

endogenous proteins (data not shown). Twelve hours after EGF stimulation, chromatin DNA from SK-N-BE cells was cross-linked and processed for ChIP assays. Sp1-derived pulled-down chromatin was amplified by a specific primer targeting the *MYCN* core promoter region (−221 to +21) in the EGF-treated cells (Fig. 4B top panel), suggesting that EGF enhances recruitment of Sp1 to the *MYCN* promoter. However, no change in E2F1 recruitment was observed between the EGF-treated and untreated cells (Fig. 4B, bottom panel).

To identify the critical Sp1-binding region required for the transactivation of *MYCN*, we mutated the Sp1-binding elements (Fig. 4C, left panel) by PCR reactions, as described in the Materials and Methods section. SK-N-BE cells were transiently transfected with wild-type *MYCN* promoter as well as the mutated luciferase constructs. Promoter assays showed that the pGL3MYCN (mut-1) construct had significantly ($P < 0.001$) less promoter activity (Fig. 4C, middle panel) than the wild type and pGL3MYCN (mut-2) constructs. Furthermore, we transiently transfected the wild type, as well as the Sp1 site 1-deleted constructs, into the SK-N-BE cells to determine the effects on EGF. The data showed that the deletion construct failed to respond to EGF treatment (Fig. 4C, right panel), suggesting that the Sp1-binding element 1 is important for EGF-mediated transactivation of *MYCN*.

To check whether Sp1 is critical for the expression of MYCN, we knocked down *Sp1* using siRNAs. Consistently, *MYCN* expression was suppressed in cells transfected with siRNAs against *Sp1* (Supplementary Fig. S2A). Both siRNAs against *Sp1* reduced *MYCN* promoter activity (Supplementary Fig. S2B). Cell proliferation was also suppressed in the *Sp1* knockdown cells (Supplementary Fig. S2C). It has been reported that EGF stimulation induces phosphorylation of ERK, and that this phosphorylation event may be important for Sp1 phosphorylation (33) and recruitment to the target gene promoter. Similarly, our results also showed that EGF treatment resulted in phosphorylation of Sp1, and this phosphorylation event was inhibited in U0126- and calf intestinal phosphatase (CIAP)-treated cells (Supplementary Fig. S3A). CIAP treatment is reported to block recruitment of phosphotranscriptional factors on genomic DNA (35). We also used Mithramycin-A (Mit-A), a well-known Sp1 inhibitor (34). EGF-mediated *MYCN* induction was successfully inhibited in cells pretreated with Mit-A (Supplementary Fig. S3B) and CIAP (Supplementary Fig. S3C). Consistently, CIAP treatment also

Published OnlineFirst July 19, 2012; DOI:10.1158/0008-5472.CAN-12-0943

reduced the recruitment of Sp1 to the *MYCN* promoter (Supplementary Fig. S3D). Collectively, our results suggest that Sp1 recruitment to the *MYCN* promoter can enhance the transactivation of *MYCN* upon EGF treatment.

NLRR1 enhances *MYCN* induction

ERK is reported to induce phosphorylation of Sp1 (33). In our present findings, NLRR1 promotes phosphorylation of ERK upon EGF treatment, suggesting that NLRR1 may induce *MYCN*. Therefore, we overexpressed NLRR1 in SK-N-BE cells and found that endogenous *MYCN* was effectively induced in a dose-dependent manner (Fig. 5A, left panel). NLRR1-mediated *MYCN* induction was inhibited in U0126- and AG1478-pretreated cells (Fig. 5A, right panel), suggesting that NLRR1 induced *MYCN* via EGFR-ERK signaling. Ectopic expression of NLRR1 in cells accelerated *MYCN* induction upon EGF treatment compared with that of mock-transfected (empty pcDNA3.1 vector) cells (Fig. 5B, left panel). Consistent with the overexpression study, knockdown of *NLRR1* suppressed *MYCN* induction, suggesting that NLRR1 accelerates EGF-mediated *MYCN* induction. To determine whether NLRR1 enhances Sp1 recruitment, we performed ChIP assays. The data show that overexpression of NLRR1 in SK-N-BE cells increased Sp1 recruitment to the *MYCN* promoter, which was further accelerated upon EGF treatment (Fig. 5C).

Stable expression of NLRR1 in cells accelerates tumor growth in nude mice

NLRR1 is highly expressed in aggressive *MYCN*-amplified neuroblastoma (14), suggesting the possibility that NLRR1 may have a potent tumorigenic role. NLRR1 overexpression enhanced the colony formation ability of SH-SY5Y cells (Supplementary Fig. S4A). Consistent with our previous observation that ectopic expression of NLRR1 enhanced cell proliferation and inhibited apoptosis, NLRR1-stably expressing SH-SY5Y clones proliferated faster than mock stable clones (Supplementary Fig. S4C). Furthermore, *MYCN* expression was upregulated in NLRR1 stable clones compared with mock clones (Supplementary Fig. S4B), suggesting that NLRR1 has oncogenic potential. To elucidate the tumorigenic activity of NLRR1, we performed tumor xenograft studies in nude mice using NLRR1-stably expressing SH-SY5Y clones. Significant enhancement of tumor growth was observed in mice bearing NLRR1-expressing xenografts compared with the mock-expressing xenografts ($P < 0.01$; Fig. 6A). Mice of each group were sacrificed when they become morbid, and the survival curve was analyzed using the Kaplan–Meier method. The survival of mice with NLRR1-expressing xenografts was significantly shorter compared with mice-bearing mock xenografts ($P = 0.003$; Fig. 6B). Immunohistochemical data showed that NLRR1-expressing tumors had increased numbers of Ki-67–positive cells and decreased number of terminal deoxynucleotidyl transferase–mediated dUTP nick end labeling (TUNEL) positive cells compared with mock tumors (Fig. 6C), indicating that there were more proliferative cells in the tumors derived from NLRR1-expressing clones. To see the consistence *in vitro* finding of NMYC induction by NLRR1, we carried out IHC assays using the tumor xenografts. Induction of NMYC and p-ERK was found in NLRR1 tumors whereas total ERK was unchanged in both tumors (Fig. 6D). Collectively, our data suggest that NLRR1 induces NMYC *in vivo* and has potent tumorigenic roles.

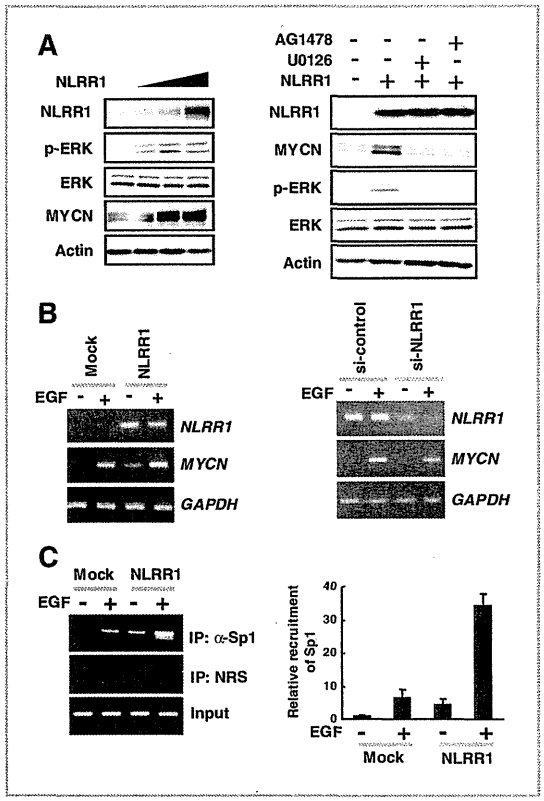

Figure 5. NLRR1 induces MYCN in neuroblastoma cells. A, SK-N-BE cells were transiently transfected with increasing amounts of NLRR1-expressing plasmids. Forty-eight hours after transfection, immunoblotting was carried out to detect NLRR1, p-ERK, total ERK, and MYCN expression (left). EGFR and ERK inhibitors prevent MYCN induction in the NLRR1-overexpressing cells. SK-N-BE cells were transiently transfected with NLRR1 expression plasmids for 48 hours and then treated with or without AG1478 (20 μmol/L) and U0126 (10 μmol/L). Twelve hours after treatment, whole cell lysates were prepared. Immunoblotting data show the expression of NLRR1, p-ERK, total ERK, and MYCN (right). B, NLRR1 enhances *MYCN* induction upon EGF treatment. Twenty-four hours after ectopic expression of NLRR1, SK-N-BE cells were cultured in serum-free medium for 12 hours followed by EGF (10 ng/mL) treatment. RT-PCR was performed to check endogenous *MYCN* expression (left). Forty hours after transfection with control siRNA and NLRR1-siRNA, SK-N-BE cells were serum starved for 12 hours and treated with EGF (10 ng/mL). Twelve hours after EGF treatment, RT-PCR was carried out to check the expression of *NLRR1* and *MYCN* (right). C, crossed-linked chromatin from the SK-N-BE mock- and NLRR1-ectopically expressing cells treated with or without EGF (50 ng/mL) for 12 hours was used for pulldown by Sp1-specific antibody. Primers targeting *MYCN* core promoter (−221, +21) were used to amplify the pulled-down chromatin (left). The recruitment of Sp1 was quantified from the PCR band by image J software and plotted (right). The data represent mean ± SD.

Published OnlineFirst July 19, 2012; DOI:10.1158/0008-5472.CAN-12-0943

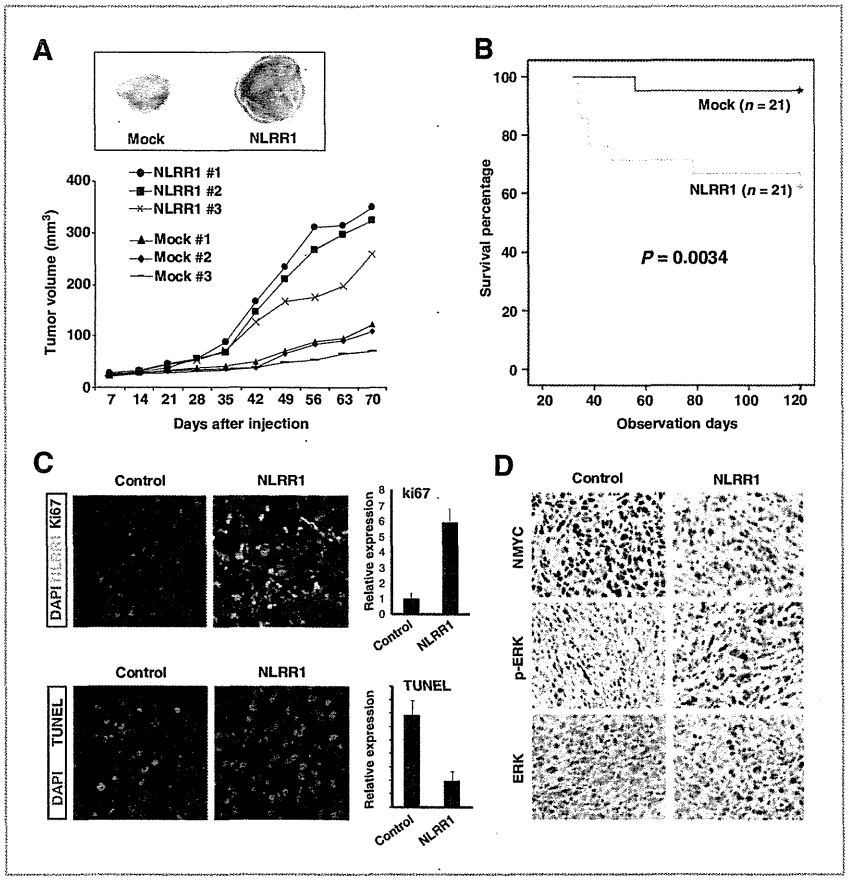

Figure 6. Neuroblastoma cells stably expressing NLRR1 accelerate tumor growth in nude mice. A, after subcutaneous injection of mock- and NLRR1-stably expressing SH-SY5Y clones into nude mice, tumor volumes were measured on the indicated days. The data represent the mean value. Top panel shows representative pictures of tumors 70 days after injection. B, Kaplan–Meyer survival curve of mice-bearing mock- and NLRR1-stably expressing SH-SY5Y xenografts. C, detection of NLRR1 and Ki-67 expression in the mock- and NLRR1-expressing tumor xenografts (top). TUNEL staining shows that NLRR1 tumor has reduced apoptotic cells (bottom). D, IHC data show the staining image of NMYC, p-ERK, and ERK in NLRR1 versus control tumors.

Discussion

Upregulated MKK-ERK signaling is known to be involved in the genesis of several cancers (18–21). Multidrug-resistant human neuroblastoma cells have three- to 30-fold more cell surface EGFRs than the drug-sensitive parental cells (36), indicating that EGFRs may play an important role in the aggressiveness of human neuroblastoma. EGF stimuli activated MAPK in neuroblastoma (16) and IGF-1 enhanced neuroblastoma cell proliferation via activation of MAPK (17). NLRR family proteins are considered to modulate cellular signaling, especially that of MAPKs (15). Although it was reported that overexpression of NLRR1 enhances cell proliferation and inhibits cellular apoptosis in neuroblastoma, our previous study did not rule out the involvement of NLRR1 with EGF and IGF-1 signaling. Here, we first report that ectopic expression of NLRR1 also enhanced EGF- and IGF-1–mediated cellular proliferation, which is inhibited in cells treated with MEK1/2 inhibitor. This suggests that NLRR1-mediated promotion of proliferation is at least in part dependent on activation of ERK. However, the method by which NLRR1 enhances EGFR and IGFR signaling still needs to be clarified. Another NLRR family protein, NLRR3, was reported to induce phosphorylation of ERK in response to EGF (15), suggesting the possibility that NLRR1 that is 54% homology to NLRR3 may also induce ERK phosphorylation. Our results propose that NLRR1 is important in enhancing ERK phosphorylation in cells upon EGF and IGF stimuli. Interestingly, NLRR1 affects p-ERK and p-AKT in different extent (Fig. 2B) that depends on cell lines (data not shown). The reason behind this selectivity is unknown and need to be addressed further in the future.

ERK is known to phosphorylate many transcriptional factors, including Sp1 (33, 37). Moreover, Sp1 and E2F1 are reported to transcriptionally regulate *MYCN* in neuroblastoma (31, 32). Therefore, there may be an important link between the activation of ERK and *MYCN* induction, which is further supported by the evidence that IGF-1 can induce *MYCN* via activation of MAPK (17). However, in this report of EGF-1-mediated MYCN induction, the involvement of Sp1 or E2F1 was not explained. Here, we report that EGF induces *MYCN* via the EGFR-ERK pathway. Several stimuli, including retinoic acid and TGF-β repress the *MYCN* gene, and are associated with recruited Sp1 and E2F1 and their other cofactors (31, 38). By using ChIP assays, we observed that Sp1 but not E2F1 was recruited to the *MYCN* promoter in response to EGF. However, it has been reported that the presence of Sp1 is not always sufficient to activate a transcriptionally silent *MYCN* gene (32).

Published OnlineFirst July 19, 2012; DOI:10.1158/0008-5472.CAN-12-0943

Therefore, we have further investigated whether Sp1 is important for *MYCN* induction in our experimental conditions. siRNA-mediated knockdown of *Sp1*-reduced *MYCN* expression and also inhibited cell proliferation, suggesting that Sp1-mediated *MYCN* induction regulates cell proliferation. Using luciferase reporter assays, we identified the responsive Sp1-binding element in the promoter region for *MYCN* induction. Sp1 phosphorylation is a prerequisite for the interaction with genomic DNA (33). Therefore, we also investigated whether EGF induces Sp1 phosphorylation and enhances its recruitment to the *MYCN* promoter. Western blotting data showed that EGF treatment enhanced phosphorylation of Sp1, and the MEK1/2 inhibitor U0126 inhibited this phosphorylation event, supporting the previous report that ERK induces Sp1 phosphorylation (33). Using the dephosphorylating agent CIAP, we further confirmed that phospho-Sp1 is involved in the transactivation of *MYCN* by recruitment to the genomic DNA of the *MYCN* promoter. Collectively, this evidence suggests that EGF induces *MYCN* through phospho-Sp1 recruitment to the *MYCN* promoter. However, MYCN induction by IGF-1 was not investigated in the present study, but we speculate that it may be by the same mechanism as EGF, because IGF-1 has been reported to activate MAPK in neuroblastoma.

Another new finding of our current study is that *MYCN* is induced after ectopic expression of *NLRR1* in neuroblastoma cells. Under our experimental conditions, EGF-mediated *MYCN* induction was accelerated in *NLRR1*-overexpressing cells and inhibited in *NLRR1*-knockdown cells, suggesting that NLRR1 enhances *MYCN* induction and activation of ERK. In addition, NLRR1 overexpression enhanced Sp1 recruitment to the *MYCN* promoter. We previously reported that *NLRR1* transcriptionally regulated by MYCN is highly expressed in aggressive neuroblastoma (14). *NLRR1* was also found to be highly expressed in *MYCN*-amplified tumors compared with that of *MYCN* nonamplified neuroblastoma. Therefore, we suggest that MYCN directly regulates NLRR1, and that NLRR1 further induces *MYCN* through the activation of the EGFR-ERK cascade, suggesting a positive feedback loop between NLRR1 and MYCN that may lead to aggressive neuroblastoma. To this notion, we further determined the *in vivo* tumorigenic activity of NLRR1 in *MYCN* nonamplified SH-SY5Y cells, which are well known to form tumors in nude mice (39, 40). Our results show that SH-SY5Y cells stably expressing NLRR1 rapidly proliferate in culture medium and in nude mice, and promote decreased survival rates among inoculated mice, presumably by induced endogenous *MYCN*.

In conclusion, our results provide significant evidence that that NLRR1 enhances ERK signaling to induce *MYCN*, which may play major roles in the progression of aggressive neuroblastoma. Taking note that *MYCN* highly expressing tumors are often resistant to antitumor therapies, new drug discovery blocking NLRR1-mediated ERK signaling to control *MYCN* expression may be an attractive choice in treating aggressive neuroblastoma.

Disclosure of Potential Conflicts of Interest

No potential conflicts of interest were disclosed.

Authors' Contributions

Conception and design: S. Hossain, A. Takatori, A. Nakagawara
Development of methodology: S. Hossain, A. Takatori, Y. Suenaga, T. Kamijo
Acquisition of data (provided animals, acquired and managed patients, provided facilities, etc.): S. Hossain, A. Takatori, Y. Nakamura
Analysis and interpretation of data (e.g., statistical analysis, biostatistics, computational analysis): S. Hossain, A. Takatori
Writing, review, and/or revision of the manuscript: S. Hossain, A. Nakagawara
Administrative, technical, or material support (i.e., reporting or organizing data, constructing databases): Y. Suenaga, Y. Nakamura, T. Kamijo, A. Nakagawara
Study supervision: A. Nakagawara

Acknowledgments

We thank Drs. M. Ohira, T. Ozaki, J. Akter, and K. Hasan (Chiba Cancer Center Research Institute, Chiba, Japan) for the fruitful discussion and assistance.

Grant Support

This work was supported by a Grant-in-Aid from the Ministry of Health, Labour, and Welfare for Third Term Comprehensive Control Research for Cancer (A. Nakagawara), a Grant-in-Aid for Scientific Research on Priority Areas from the Ministry of Education, Culture, Sports, Science, and Technology, Japan (A. Nakagawara), a grant from the Takeda Science Foundation, and a Grant-in-Aid for Scientific Research from the Japanese Society for the Promotion of Science (A. Takatori and A. Nakagawara).

The costs of publication of this article were defrayed in part by the payment of page charges. This article must therefore be hereby marked *advertisement* in accordance with 18 U.S.C. Section 1734 solely to indicate this fact.

Received March 16, 2012; revised May 21, 2012; accepted June 6, 2012; published OnlineFirst July 19, 2012.

References

1. Brodeur GM. Neuroblastoma: biological insights into a clinical enigma. Nat Rev Cancer 2003;3:203–16.
2. Weinstei JL, Katzenstein HM, Cohn SL. Advances in the diagnosis and treatment of neuroblastoma. Oncologist 2003;8:278–92.
3. Brodeur GM, Nakagawara A. Molecular basis of clinical heterogeneity in neuroblastoma. Am J Pediatr Hematol Oncol 1992;14:111–6.
4. Bown N, Cotterill S, Lastowska M, O'Neill S, Pearson AD, Plantaz D, et al. Gain of chromosome arm 17q and adverse outcome in patients with neuroblastoma. N Engl J Med 1999;340:1954–61.
5. Frappaz D, Michon J, Coze C, Berger C, Plouvier E, Lasset C, et al. LMCE3 treatment strategy: results in 99 consecutively diagnosed stage 4 neuroblastomas in children older than 1 year at diagnosis. J Clin Oncol 2000;18:468–76.
6. Schmidt ML, Lukens JN, Seeger RC, Brodeur GM, Shimada H, Gerbing RB, et al. Biologic factors determine prognosis in infants with stage IV neuroblastoma: a prospective Children's Cancer Group study. J Clin Oncol 2000;18:1260–8
7. Felsher DW, Bishop JM. Reversible tumorigenesis by MYC in hematopoietic lineages. Mol Cell 1999;4:199–207.
8. D'Cruz CM, Gunther EJ, Boxer RB, Hartman JL, Sintasath L, Moody SE, et al. c-MYC induces mammary tumorigenesis by means of a preferred pathway involving spontaneous Kras2 mutations. Nat Med 2001;7:235–9.
9. Pelengaris S, Littlewood T, Khan M, Elia G, Evan G. Reversible activation of c-Myc in skin: induction of a complex neoplastic phenotype by a single oncogenic lesion. Mol Cell 1999;3:565–77.
10. Taguchi A, Wanaka A, Mori T, Matsumoto K, Imai Y, Takagi T, et al. Molecular cloning of novel leucine-rich repeat proteins and their expression in the developing mouse nervous system. Brain Res Mol Brain Res 1996;35:31–40.

Published OnlineFirst July 19, 2012; DOI:10.1158/0008-5472.CAN-12-0943

11. Taniguchi H, Tohyama A, Takagi T. Cloning and expression of a novel gene for a protein with leucine-rich repeats in the developing mouse nervous system. Brain Res Mol Brain Res 1996;36:45–52.
12. Hamano S, Ohira M, Isogai E, Nakada K, Nakagawara A. Identification of novel human neuronal leucine-rich repeat (hNLRR) family genes and inverse association of expression of Nbla10449/hNLRR-1 and Nbla1067/hNLRR-3 with the prognosis of primary neuroblsatoma. Int J Oncol 2004;24:1457–66.
13. Bando T, Sekine K, Kobayashi S, Watabe AM, Rump A, Tanaka M, et al. Neuronal leucine-rich repeat protein 4 functions in hippocampus-dependent long-lasting memory. Mol Cell Biol 2005;25:4166–75.
14. Hossain MS, Ozaki T, Wang H, Nakagawa A, Takenobu H, Ohira M, et al. N-MYC promotes cell proliferation through a direct transactivation of neuronal leucine-rich repeat protein-1 (NLRR1) gene in neuroblastoma. Oncogene 2008;27:6075–82.
15. Fukamachi K, Matsuoka Y, Ohno H, Hamaguchi T, Tsuda H. Neuronal leucine-rich repeat protein-3 amplifies MAPK activation by epidermal growth factor through a carboxy-terminal region containing endocytosis motifs. J Biol Chem 2002;277:43549–52.
16. Ho R, Mintum JE, Hishiki T, Zhao H, Wang Q, Cnaan A, et al. Proliferation of human neuroblastomas mediated by the epidermal growth factor receptor. Cancer Res 2005;65:9868–75.
17. Misawa A, Hosoi H, Arimoto A, Shikata T, Akioka S, Matsumura T, et al. N-Myc induction stimulated by insulin-like growth factor I through mitogen-activated protein kinase signaling pathway in human neuroblastoma cells. Cancer Res 2000;60:64–9.
18. Chang L, Karin M. Mammalian MAP kinase signalling cascades. Nature 2001;410:37–40.
19. Johnson GL, Lapadat R. Mitogen-activated protein kinase pathways mediated by ERK, JNK, and p38 protein kinases. Science 2002;298: 1911–2.
20. Dunn KL, Espino PS, Drobic B, He S, Davie JR. The Ras-MAPK signal transduction pathway, cancer and chromatin remodeling. Biochem Cell Biol 2005;83:1–14.
21. Davies H, Bignell GR, Cox C, Stephens P, Edkins S, Clegg S, et al. Mutations of the BRAF gene in human cancer. Nature 2002;417: 949–54.
22. Jeffers M, Fiscella M, Webb CP, Anver M, Koochekpour S, Vande Woude GF. The mutationally activated Met receptor mediates motility and metastasis. Proc Natl Acad Sci U S A 1998;95:14417–22.
23. Webb CP, Taylor GA, Jeffers M, Fiscella M, Oskarsson M, Resau JH, et al. Evidence for a role of Met-HGF/SF during Ras-mediated tumorigenesis/metastasis. Oncogene 1998;17:2019–25.
24. Ward Y, Wang W, Woodhouse E, Linnoila I, Liotta L, Kelly K. Signal pathways which promote invasion and metastasis: critical and distinct contributions of extracellular signal-regulated kinase and Ral-specific guanine exchange factor pathways. Mol Cell Biol 2001;21: 5958–69.
25. Ghos AK, Steele R, Ray RB. Carboxy-terminal repressor domain of MBP-1 is sufficient for regression of prostate tumor growth in nude mice. Cancer Res 2005;65:718–21.
26. Konstantinidou G, Bey EA, Rabellino A, Schuster K, Maira MS, Gazdar AF, et al. Dual phosphoinositide 3-kinase/mammalian target of rapamycin blockade in an effective radiosensitizing strategy for the treatment of non-small cell lung cancer harboring K-ras mutations. Cancer Res 2009;69:7644–52.
27. Wang J, Zhou J, Wu GS. ERK-dependent MKP-1-mediated cisplatin resistance in human ovarian cancer cells. Cancer Res 2007;67: 11933–41.
28. Maity A, Pore N, Lee J, Solomon D, O'Rourke DM. Epidermal growth factor receptor transcriptionally up-regulates vascular endothelial growth factor expression in human glioblastoma cells via a pathway involving phosphatidylinositol 3′-kinase and distinct from that induced by hypoxia. Cancer Res 2000;60:5879–86.
29. Davisll JW, Lauer FT, Burdick AD, Hudson LG, Burchiel SW. Prevention of apoptosis by 2,3,7,8-Tetrachlorodibenzo-p-dioxin (TCDD) in the MCF-10A cell line: correlation with increased transforming growth factor α production. Cancer Res 2001;61:3314–20.
30. Zhou Y, Brattain MG. Synergy of epidermal growth factor receptor kinase inhibitor AG1478 and ErbB2 kinase inhibitor AG879 in human colon carcinoma cells is associated with induction of apoptosis. Cancer Res 2005;65:5848–56.
31. Strieder V, Lutz W. E2F proteins regulate MYCN expression in neuroblastomas. J Biol Chem 2003;278:2983–9.
32. Kramps C, Strieder V, Sapetschnig A, Suske G, Lutz W. E2F and Sp1/Sp3 Synergize but are not sufficient to activate the MYCN gene in neuroblastomas. J Biol Chem 2004;279:5110–7.
33. Merchant JL, Du M, Todisco A. Sp1 phosphorylation by Erk 2 stimulates DNA binding. Biochem Biophys Res Commun 1999; 254:454–61.
34. Jia Z, Zhang J, Wei D, Wang L, Yuan P, Le X, et al. Molecular basis of the synergestic sntiangiogenesis activity of Bevacizumab and Mithramycin A. Cancer Res 2007;67:4878–85.
35. Matsuoka T, Zhao L, Stein R. The DNA binding activity of the RIPE3b1 transcription factor of insulin appears to be influenced by tyrosine phosphorylation. I Biol Chem 2001;276:22071–6.
36. Meyers MB, Shen WP, Spengler BA, Ciccarone V, O'Brien JP, Donner DB, et al. Increased epidermal growth factor receptor in multidrug-resistant human neuroblastoma cells. J Cell Biochem 1988;38:87–97.
37. Milanini-Mongiat J, Pouyssegur J, Pages G. Identification of two Sp1 phohphorylation sites for p42/44 mitogen-activated protein kinases. J Bio Chem 2002;277:20631–9.
38. Ferreira R, Naguibneva I, Pritchard LL, Ait-Si-Ali S, Harel-Bellan A. The Rb/chromatin connection and epigenetic control: opinion. Oncogene 2001;20:3128–33.
39. Aoyama M, Ozaki T, Inzuka H, Tomotsune D, Hirato J, Okamoto Y, et al. LMO3 interacts with neuronal transcription factor, HEN2, and acts as an oncogene in neuroblastoma. Cancer Res 2005:65:4587–97.
40. Eggert A, Grotzer MA, Ikegaki N, Liu XG, Evans AE, Brodeur GM. Expression of the neurotrophin receptor TrkA down-regulates expression and fuinction of angiogenic stimulators in SH-SY5Y neuroblastoma cells. Cancer Res 2002;62:1802–8.

A noncoding RNA regulates the neurogenin1 gene locus during mouse neocortical development

Masahiro Onoguchi[a], Yusuke Hirabayashi[a], Haruhiko Koseki[b], and Yukiko Gotoh[a,1]

[a]Institute of Molecular and Cellular Biosciences, University of Tokyo, Tokyo 113-0032, Japan; and [b]RIKEN Center for Allergy and Immunology, Kanagawa 230-0045, Japan

Edited by Michael Eldon Greenberg, Harvard Medical School, Boston, MA, and approved September 5, 2012 (received for review February 20, 2012)

The proneural basic helix–loop–helix (bHLH) transcription factor neurogenin1 (Neurog1) plays a pivotal role in neuronal differentiation during mammalian development. The spatiotemporal control of the *Neurog1* gene expression is mediated by several specific enhancer elements, although how these elements regulate the *Neurog1* locus has remained largely unclear. Recently it has been shown that a large number of enhancer elements are transcribed, but the regulation and function of the resulting transcripts have been investigated for only several such elements. We now show that an enhancer element located 5.8–7.0 kb upstream of the mouse *Neurog1* locus is transcribed. The production of this transcript, designated *utNgn1*, is highly correlated with that of *Neurog1* mRNA during neuronal differentiation. Moreover, knockdown of *utNgn1* by a corresponding short interfering RNA inhibits the production of *Neurog1* mRNA in response to induction of neuronal differentiation. We also found that production of *utNgn1* is suppressed by polycomb group (PcG) proteins, which inhibit the expression of *Neurog1*. Our results thus suggest that a noncoding RNA transcribed from an enhancer element positively regulates transcription at the *Neurog1* locus.

The mammalian central nervous system (CNS) is composed of a great variety of neurons and glial cells, all of which must be generated from multipotential neural precursor cells (NPCs) in the correct number and at specific times and locations during embryogenesis (1, 2). Proneural basic helix–loop–helix (bHLH) proteins play central roles in the specification of neuronal fate and the subsequent differentiation processes (3). Among these proteins, neurogenin1 (Neurog1) is a key regulator of neuronal fate specification in various regions of the neural tube, including those that give rise to the neocortex, midbrain, hindbrain, and dorsal and ventral spinal cord of the CNS, as well as in portions of the peripheral nervous system (4–7). In the developing mouse neocortex, ablation of *Neurog1* along with the related protein neurogenin2 (Neurog2) results in the loss of deep-layer neurons (8), and conversely, overexpression of *Neurog1* results in premature neuronal differentiation of NPCs at the expense of glial fate (9, 10). These observations suggest that expression of the *Neurog1* and *Neurog2* genes must be tightly controlled in a spatiotemporal manner during development to ensure the generation of specific subsets of neurons and establishment of the fine architecture of the CNS.

Spatiotemporal control of gene expression is generally mediated by regulatory elements including enhancers. Previous studies have revealed several enhancer elements that control expression of the *Neurog1* gene, including the lateral stripe element (LSE), the anterior neural plate element (ANPE), and the LATE; which were originally identified as tissue-specific enhancers in zebrafish and found to be conserved among various vertebrate genomes including the mouse genome (11–13). Deletion of the 4-kb mouse genomic region including LATE and ANPE significantly reduced overall expression of *Neurog1* in a transgenic reporter assay (14). Therefore, although this 4-kb region has been implicated in tissue-specific regulation, it might also contain an essential general enhancer or locus control region. It has remained elusive, however, how these regions regulate *Neurog1* expression and how their activity is regulated.

Several molecules have been implicated in the regulation of *Neurog1* expression during neocortical development. For instance, Wnt signaling induces expression of *Neurog1* via β-catenin and T cell specific transcription factor (TCF)/lymphoid enhancer binding factor (LEF) transcription factors in neocortical NPCs (15, 16). The homeodomain transcription factor Pax6, which contributes to neocortical regional identity, also positively regulates expression of *Neurog1* (12, 17). In contrast, Polycomb group (PcG) proteins suppress the *Neurog1* promoter during the gliogenic stage of neocortical development when the neurogenic potential of NPCs is restricted (18). Whether or how these molecules affect the enhancers of *Neurog1* has remained unclear.

Various mechanisms have been proposed for the regulation of a gene by a corresponding enhancer (19). Classically, enhancers are viewed as clusters of DNA elements that bind transcription factors, which in turn interact with the mediator complex or transcription factor IID to facilitate the recruitment of RNA polymerase II (as well as that of chromatin modifying enzymes) to the promoter region through "DNA looping" (20). However, recent studies have indicated that enhancer sequences are not simply binding sites for transcription factors and cofactors; rather, many of them are also transcribed to generate noncoding RNAs when the transcription of corresponding genes takes place (21–26). The functions of such enhancer-associated noncoding RNAs have only just begun to be elucidated, such as in the case of those derived from the Snail1 and HoxA gene loci (23–25).

In this study, we found that an enhancer region spanning from between LATE and ANPE to LATE is transcribed in mouse neocortical NPCs and that expression of this transcript (designated *utNgn1*) correlates well with that of *Neurog1* mRNA. Knockdown experiments revealed that *utNgn1* is necessary for the effective transcription of *Neurog1* in neocortical NPCs, suggesting that one of the enhancers of the *Neurog1* locus functions via generation of its transcript. Furthermore, the amount of *utNgn1* was found to be increased by Wnt signaling and to be down-regulated by PcG proteins. We noticed that the *utNgn1* locus in neocortical NPCs harbors histone H3 lysine 27 trimethylation (H3K27me3), a histone mark catalyzed by PcG proteins, as well as histone H3 lysine 4 trimethylation (H3K4me3) and histone H3 lysine 9 or 14 acetylation (H3K9/K14ac), marks of active transcription (27). Our results thus suggest that the enhancer of *Neurog1* regulates the expression of *Neurog1* via its transcript, and PcG proteins suppress a target gene not only directly by occupying promoter regions but also indirectly by occupying their enhancers.

Results

***utNgn1* Is Transcribed from an Enhancer Region of the *Neurog1* Locus.** A 4-kb region located 3.8–7.8 kb upstream of the transcription start site (TSS) of mouse *Neurog1* has been implicated in regulation of *Neurog1* expression in most expression domains of the mouse embryo (14), suggesting the existence of a general enhancer within this region. Given that this region contains a CpG island (CGI) between ANPE and LATE (Fig. 1*A*), we hypothesized that it might be transcriptionally active (28). We therefore first examined

Author contributions: M.O., Y.H., and Y.G. designed research; M.O. and Y.H. performed research; H.K. contributed new reagents/analytic tools; M.O., Y.H., and Y.G. analyzed data; and M.O., Y.H., and Y.G. wrote the paper.

The authors declare no conflict of interest.

This article is a PNAS Direct Submission.

[1]To whom correspondence should be addressed. E-mail: ygotoh@iam.u-tokyo.ac.jp.

This article contains supporting information online at www.pnas.org/lookup/suppl/doi:10.1073/pnas.1202956109/-/DCSupplemental.

whether the region surrounding this CGI contains the H3K4me3 mark, which is associated with the promoters of actively transcribed genes (or genes in a state permissive for transcription). We cultured NPCs prepared from the mouse neocortex at embryonic day (E) 11.5 for 3 d in vitro (DIV) as neurospheres (E11.5 + 3DIV culture). Chromatin immunoprecipitation (ChIP) assay revealed the presence of this modification in the region ~7 kb upstream of the TSS of *Neurog1* (Fig. 1*A*, primer 5), with a peak in H3K4me3 at the CGI (Fig. 1*B*). The amount of H3K4me3 at the CGI was similar to that at the promoter of *Neurog1* as well as at the promoter of the actively transcribed gene *Gapdh*, suggesting that the region surrounding the CGI might be transcribed. This notion was further supported by the observation that H3K9/K14ac, another histone modification associated with actively transcribed genes, was also present in the region surrounding the CGI (Fig. 1*C*).

We next performed RT-PCR analysis to search for transcripts derived from the region surrounding the CGI and detected PCR amplicons originating from a position ~6.1 kb upstream of the TSS of *Neurog1* in the mouse neocortex at E13.5 (Fig. 1 *A* and *D*). Furthermore, quantitative RT-PCR (qRT-PCR) analysis revealed that a significant level of transcription occurs in this position compared with other intergenic regions such as ~1.2, 3.6, and 4.6 kb upstream of the TSS of *Neurog1* (Fig. 1 *A* and *E*). Next, to determine the 5′ and 3′ ends of the transcripts, we performed rapid amplification of cDNA ends (RACE) analysis (Fig. 1*F*). 5′ RACE revealed multiple 5′ ends within the CGI, consistent with previous observations showing that CGI promoters are accompanied by multiple initiation points within the CGI (*29*). 3′ RACE revealed a polyadenylation signal at position −5.8 kb relative to the TSS of *Neurog1*. Consistent with these observations, Northern blot analysis with an antisense probe corresponding to positions −6.0 to −6.4 kb revealed a transcript of ~1.4 kb in a total RNA fraction isolated from the mouse neocortex at E13.5 (Fig. 1*G*). We now refer to this transcript derived from an enhancer region of *Neurog1* as *utNgn1* (upstream transcript of the *Neurog1* locus). The longest ORF of *utNgn1* potentially encodes a 49-amino-acid protein with

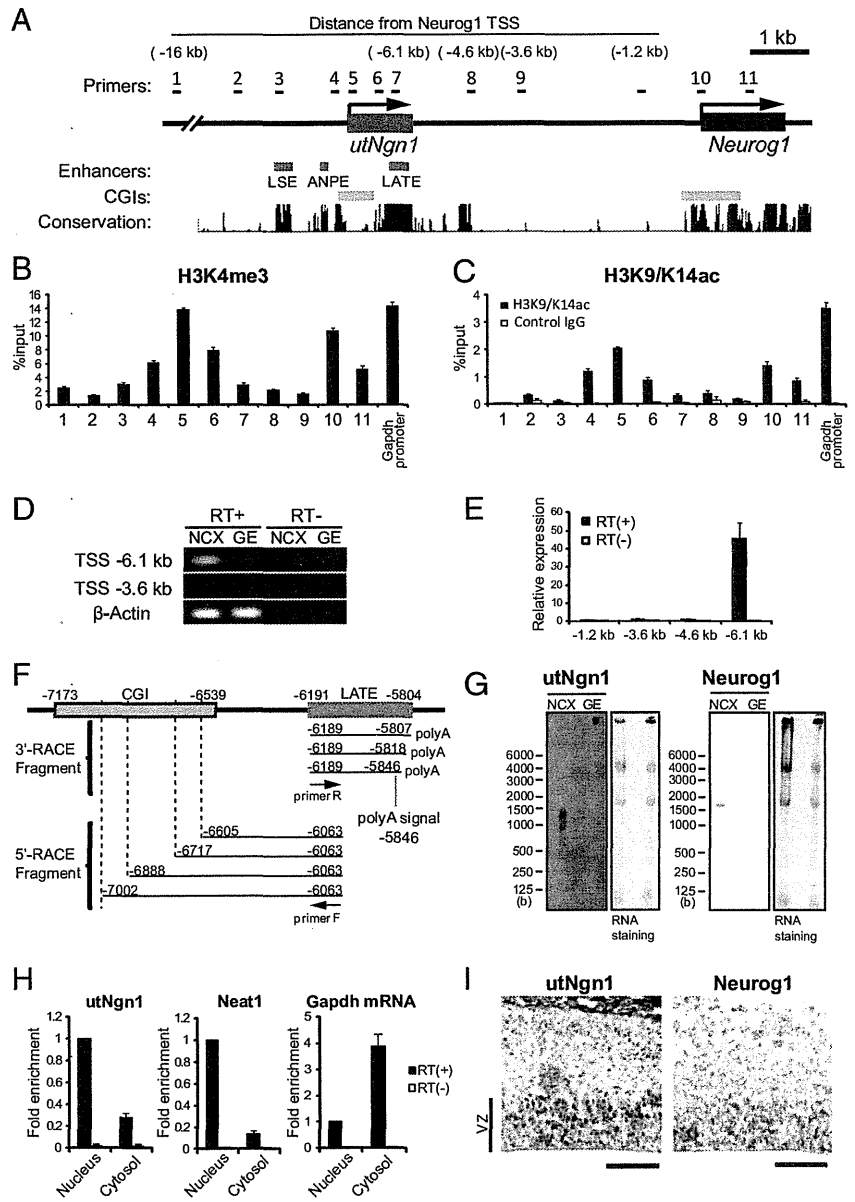

Fig. 1. A noncoding RNA, *utNgn1*, is transcribed from an enhancer region of *Neurog1*. (*A*) Schematic representation of enhancers and CpG islands (CGIs) of the mouse *Neurog1* locus. Blue and green boxes indicate enhancers (LATE, ANPE, and LSE) identified in zebrafish and CGIs, respectively. Black arrows indicate the direction of transcription of *utNgn1* (red box) and *Neurog1* (black box). Conservation plot and CGIs are adapted from the University of California Santa Cruz Genome Browser. Black bars indicate the positions of PCR primers used for RT-PCR or ChIP analysis. (*B* and *C*) Primary NPCs isolated from the E11.5 mouse neocortex (NCX) were cultured in suspension for 3DIV in the presence of fibroblast growth factor 2 (FGF2) and epidermal growth factor (EGF). Cells were then subjected to ChIP analysis with antibodies to H3K4me3 (*B*) or H3K9/K14ac (or with control IgG) (*C*) and with the PCR primers indicated in *A* or those specific for the promoter of *Gapdh*. Data are expressed as percentage of the input and are means ± SEM for three samples. (*D*) Total RNA extracted from the NCX or ganglionic eminences (GE) of E13.5 mouse embryos was subjected to RT (or not) with an oligo (dT) primer followed by PCR with primers targeted to regions located 6.1 kb or 3.6 kb upstream of the transcription start site (TSS) of *Neurog1* as well as with those specific for β-actin (internal control). (*E*) Relative expression levels of *utNgn1* locus (*Neurog1* TSS −6.1 kb) in the neocortex compared with other intergenic regions (*Neurog1* TSS −1.2, −3.6, and −4.6 kb) are determined by qRT-PCR. Data represent means ± SEM from three embryos at E13.5. (*F*) 5′ and 3′ RACE analysis of *utNgn1* with cDNA prepared from poly(A)$^+$ or total RNA of the mouse neocortex at E12.5. Black arrows indicate PCR primers F and R. Four 5′ ends and three 3′ ends were determined by DNA sequencing in 5′ RACE and 3′ RACE, respectively. Amplified fragments are mapped on the *Neurog1* upstream region, and a polyadenylation signal (AAATAA) is shown. (*G*) Northern blot analysis of total RNA prepared from the E13.5 NCX or GE were performed with DIG-labeled RNA probes specific for *utNgn1* or *Neurog1* mRNA. Blots were also stained with SYBR Gold (*Right*). (*H*) Relative concentration of *utNgn1* in the nuclear and cytosolic fractions. Cells were prepared from the E12.5 mouse NCX and cultured in suspension for 3DIV. The same amount of total RNA extracted from nuclear or cytosolic fractions of NPCs were reverse transcribed. Relative amounts of the cDNA in each fraction were determined by qRT-PCR. Data are expressed relative to the corresponding value for concentration in the nuclear fraction and are means ± SEM from three independent experiments. (*I*) In situ hybridization analysis of *utNgn1* and *Neurog1* mRNA in coronal sections of the E13.5 mouse NCX. VZ, ventricular zone. (Scale bar, 50 μm.)

no sequence similarity to any expressed sequences currently deposited in protein databases. Moreover, it may not be translated because fractionation of neocortical NPCs (E12.5 + 3DIV culture) revealed that the concentration of *utNgn1* is higher in the nucleus compared with the cytosol, which is characteristic of noncoding RNA (for instance, *Neat1*, *Malat1*, or *Xist*) (30) in contrast to the cytosol-enriched localization of coding RNA (mRNA) (Fig. 1*H*). We cannot, however, exclude the possibility that *utNgn1* is translated. Although *utNgn1* and *Neurog1* mRNA are encoded on the same strand, they do not appear to be components of the same transcript, given that neither the probe for *utNgn1* nor one for *Neurog1* mRNA detected a transcript spanning both target RNAs (>3 kb) in Northern blot analysis (Fig. 1*G*). In addition, we could not detect a transcript, by qRT-PCR, or association with histone H3 lysine 36 trimethylation (H3K36me3) (27), by ChIP analysis, for the region between the coding sequences for *utNgn1* and *Neurog1* mRNA (Fig. 1*E* and Fig. S1).

Correlation Between *utNgn1* and *Neurog1* mRNA Expression Patterns. Long noncoding RNAs have previously been found to affect gene expression both positively and negatively (31). We therefore compared the expression pattern of *utNgn1* with that of *Neurog1* mRNA. We isolated various regions of the developing CNS, including the neocortex, ganglionic eminences, diencephalon, midbrain, hindbrain, and spinal cord, as well as nonneural tissues, including the heart, liver, and limb, from mouse embryos at E13.5. qRT-PCR analysis revealed that *utNgn1* was expressed in all regions of the CNS that expressed *Neurog1* mRNA, but neither RNA was detected in the nonneural tissues (Fig. 2*A*) (14). Moreover, the amount of *utNgn1* correlated well with that of *Neurog1* mRNA. The expression level of *utNgn1* is very low (1/30–1/300 of that of *Neurog1*) (Fig. 2 *A–D*). Northern blot analysis also showed that both *utNgn1* and *Neurog1* mRNA were more abundant in the neocortex than in the ganglionic eminences (Fig. 1*G*). These results thus suggested that the expression of *utNgn1* is positively correlated with that of *Neurog1* mRNA.

We also examined the expression of *utNgn1* by in situ hybridization. An antisense probe for *utNgn1* yielded robust signals in a subpopulation of cells located within the ventricular zone (which contains NPCs) of the E13.5 mouse neocortex (Fig. 1*I*), the midbrain, and a dorsal part of the diencephalon (Fig. S2 *A* and *B*). Importantly, the expression pattern of *utNgn1* largely overlapped with that of *Neurog1* mRNA, providing further support for a positive correlation between *utNgn1* and *Neurog1* mRNA expression in the developing CNS.

We next asked whether the expression level of *utNgn1* changes during neuronal differentiation of neocortical NPCs. NPCs freshly prepared from the neocortex at E11.5 were maintained in an undifferentiated state in the presence of fibroblast growth factor (FGF)2. Removal of FGF2 in such primary cultures results in neuronal differentiation and promotes the production of *Neurog1* mRNA and subsequently that of *βIII-tubulin* mRNA (32) (Fig. 2*B*). Here we found that, under the same conditions, growth factor deprivation also induced expression of *utNgn1* with a time course similar to that of *Neurog1* mRNA (Fig. 2*B*), indicating that the expression of *utNgn1* positively correlates with that of *Neurog1* mRNA and is induced during an early phase of neuronal differentiation of neocortical NPCs.

We next investigated how the production of *utNgn1* is regulated by extracellular signals, which regulate neuronal differentiation of NPCs. Notch signaling is essential for the maintenance of undifferentiated state of NPCs and suppress neuronal differentiation. We then induced neuronal differentiation of NPCs by treatment with *N*-[*N*-(3,5-difluoro-phenacetyl)-L-alanyl]-(*S*)-phenylglycine *t*-butyl ester (DAPT), a presenilin inhibitor that suppresses Notch signaling and thereby reduces the amount of *Hes1* and *Hes5* mRNA, a downstream effector of Notch signaling (33) (Fig. 2*C*). Exposure of the NPC cultures to DAPT induced the expression of *utNgn1* and that of *Neurog1* mRNA (Fig. 2*C*). Wnt signaling is another extracellular signaling that regulates neuronal differentiation and *Neurog1* expression in the mouse neocortex. We therefore examined whether Wnt signaling might also regulate *utNgn1* expression. Treatment of E11.5 neocortical NPCs with recombinant Wnt3a for 9 or 24 h increased the amounts of *utNgn1* and of *Neurog1* mRNA (Fig. 2*D*). These results further indicate that the expression of *utNgn1* positively correlates with that of *Neurog1* mRNA and is induced during neuronal differentiation of neocortical NPCs.

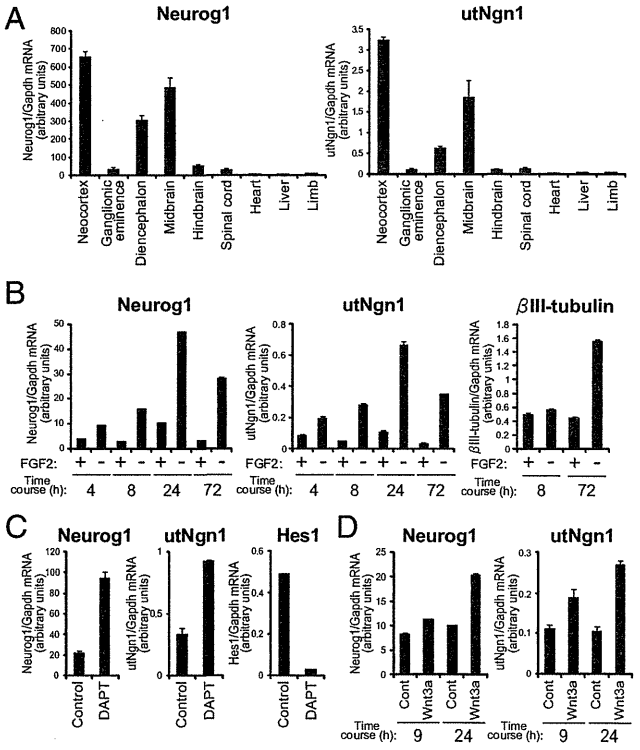

Fig. 2. Expression pattern of *utNgn1* is highly correlated with that of *Neurog1* mRNA. (*A*) Tissues were isolated from the neocortex, ganglionic eminences, diencephalon, midbrain, hindbrain, spinal cord, heart, liver, and limb of E13.5 mouse embryos. (*B*) Primary NPCs prepared from the E11.5 neocortex were cultured for 1 d and then incubated for the indicated times in medium with or without FGF2. (*C*) Primary NPCs prepared from the E11.5 neocortex were cultured for 2 d and then exposed to DAPT (5 μM) or dimethyl sulfoxide vehicle (control) for 7 h. (*D*) Primary NPCs prepared from the E11.5 neocortex were cultured without (control) or with Wnt3a for 9 or 24 h. (*A–D*) Total RNA was isolated from the cells or tissues and subjected to qRT-PCR analysis of each gene. Relative amounts of *Neurog1* and *utNgn1* were determined using a standard curve derived from a BAC clone, which contained both *Neurog1* and *utNgn1* loci, making the values of *Neurog1* and *utNgn1* transcripts comparable. Data are normalized by the amount of *Gapdh* mRNA and are means ± SEM (n = 3).

We also examined the expression of *utNgn1* in embryonic stem (ES) cells and ES-derived NPCs (Fig. S3) (34). Neither *utNgn1* nor *Neurog1* mRNA was detected in ES cells in the undifferentiated state (day 0), but both transcripts were found to be expressed after culturing the cells for 7 d under conditions that induce differentiation into NPCs (day 7). Again, these results supported a positive correlation between transcription of *utNgn1* and that of *Neurog1* mRNA during development.

***utNgn1* Positively Regulates *Neurog1* Expression.** Transcription of neighboring loci can be positively correlated as a result of the phenomenon known as transcriptional noise or "ripples" (35), which might be dependent on mechanisms including chromatin remodeling. We therefore investigated whether *utNgn1* functions in gene regulation or is simply a byproduct of *Neurog1* expression. To assess its possible role in *Neurog1* expression, we knocked down *utNgn1* in E11.5 NPCs using small interfering RNAs (siRNAs) targeted to three different sequences within *utNgn1* and three control siRNAs. Growth factor deprivation for 10 h induced *Neurog1* expression in cells without siRNA or with control siRNA, but this effect was markedly inhibited in cells harboring any of the

siRNAs specific for *utNgn1* (Fig. 3*A* and Fig. S4). We confirmed that the nuclear level of *utNgn1* was effectively decreased by siRNAs targeting *utNgn1* (Fig. 3*B*). We examined the expression of genes within 1 Mb of the *utNgn1* locus and found that knockdown of *utNgn1* did not reduce the expression of any of these genes except for *Neurog1* (Fig. 3*C* and Fig. S5 *A* and *B*). We also found that depletion of *Neurog1* mRNA with a corresponding siRNA did not affect the amount of *utNgn1* (Fig. 3*D*). These results thus suggest that *utNgn1* is not simply a byproduct of transcription of a neighboring gene, but rather is a positive regulator of *Neurog1* expression, providing an example of gene regulation through the production of an enhancer-derived transcript.

Next we examined the biological function of *utNgn1*. Consistent with the proposed role of *Neurog1* in neuronal fate commitment in neocortical NPCs (8), we found that *utNgn1* knockdown partially inhibited the induction of *Tbr2* and *NeuroD1*, early markers of neocortical neuronal fate commitment, under a differentiation-inducing condition (Fig. S5*C*). Therefore, *utNgn1* might play a role in neuronal fate commitment of these cells.

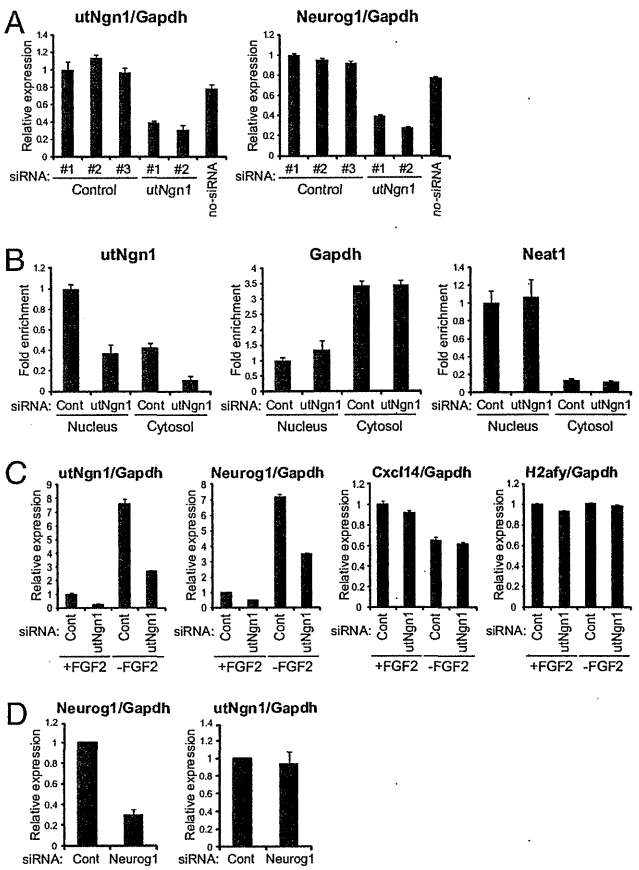

Fig. 3. *utNgn1* is required for the expression of *Neurog1* during neuronal differentiation. (*A*, *C*, and *D*) Primary NPCs prepared from the E11.5 neocortex were transfected with three independent control (siRNAs 1, 2, and 3), two independent siRNAs against *utNgn1* (*utNgn1* siRNA 1 and 2), or without siRNAs (no-siRNA) (*A*). Similarly, cells were transfected with control (siRNA 1), *utNgn1* (siRNA 1), or siRNA against *Neurog1* (*C* and *D*). Cells were cultured for 2 d with FGF2 and then for 10 h with or without FGF2. Total RNA was then extracted from the cells and subjected to qRT-PCR analysis of each gene. Data are normalized with the amount of *Gapdh* mRNA, are expressed relative to the corresponding value for cells transfected with the control siRNA 1, and are means ± SEM ($n = 3$). (*B*) Primary NPCs prepared from the E11.5 neocortex were transfected with a control (siRNA 1) or with a combination of two independent siRNAs against *utNgn1* (*utNgn1* siRNAs 1 and 2). Cells were cultured for 3 d in suspension with FGF2 and EGF, harvested and fractionated, as described in Fig. 1*H*, and the amount of RNA in each fraction was determined.

***utNgn1*, but Not Its Truncated Form, Positively Regulates Expression of Its Downstream Gene.** To investigate whether *utNgn1* is capable of *cis*-regulating the transcription of its downstream gene, we performed a reporter gene assay. We designed Firefly luciferase (luc2) reporter constructs as schematized in Fig. 4*A*. In these constructs, the luc2 gene is under the control of the *Neurog1* promoter either alone (*a*), with an intact *utNgn1* (*b*), or with a truncated *utNgn1* harboring early termination sequences (*c*). In vector *c*, we inserted early termination sequences in *utNgn1* between the CGI and the LATE enhancer to inhibit the expression of full-length *utNgn1* without affecting the LATE enhancer sequence itself. A synthetic poly(A) signal transcriptional pause site was inserted between *utNgn1* and the *Neurog1* promoter to prevent the direct effect of upstream transcription on reporter transcription. We found that the insertion of *utNgn1* into an upstream region of the *Neurog1* promoter significantly enhanced reporter gene transcription (Fig. 4*B*). Importantly, insertion of early termination sequences in *utNgn1* resulted in a loss of the increased reporter gene expression, suggesting the importance of an intact *utNgn1* transcript for this action (Fig. 4*B*). This result provides additional evidence indicating the importance of *utNgn1* for *Neurog1* gene transcription.

PcG Proteins Suppress *utNgn1* Expression. During the late stage of neocortical development, which is associated with the restriction of neuronal fate and activation of the gliogenic phase of NPCs, PcG proteins suppress the *Neurog1* promoter (18). We therefore asked whether PcG proteins also regulate *utNgn1* expression. ChIP analysis with neocortical NPCs (E11.5 + 3DIV or 9DIV) revealed that the *utNgn1* locus was broadly occupied by H3K27me3, a histone mark catalyzed by PcG proteins, at levels comparable to those at the promoter of *Neurog1* (Fig. 5*A*). Therefore, like the *Neurog1* locus, the *utNgn1* locus is also "bivalent," harboring both H3K4me3 (active) and H3K27me3 (repressive) histone marks (36). Neocortical E11.5 + 3DIV and E11.5 + 9DIV NPC cultures are characterized by preferential differentiation into neurons and astrocytes, respectively, under the conditions adopted in the present study (18). The level of H3K27me3 at the *utNgn1* locus was substantially higher in E11.5 + 9DIV cultures than in E11.5 + 3DIV cultures (Fig. 5*A*), suggesting that this change is associated with the late (gliogenic) stage of neocortical NPC development. In contrast, the level of H3K4me3 at both *utNgn1* and *Neurog1* loci remained largely unchanged between E11.5 + 3DIV and E11.5 + 9DIV (Fig. 5*B*).

The high levels of H3K27me3 at the *utNgn1* locus suggest that PcG proteins may suppress the production of the enhancer-encoded transcript during the late developmental stage of neocortical NPCs. To test this hypothesis, we first examined whether the expression of *utNgn1* is indeed repressed in the late stage of neocortical NPC development. The level of *utNgn1*, as well as that of *Neurog1* mRNA, was greatly reduced in E11.5 + 9DIV cultures compared with that in E11.5 + 3DIV cultures (Fig. 5*C*). We observed similar reductions of both *utNgn1* and *Neurog1* in E17.5 + 3DIV cultures relative to E11.5 + 3DIV cultures (Fig. 5*C*), suggesting that the suppression of *utNgn1* expression is the result of developmental progression rather than culture duration. Consistent with this, the expression levels of both *Neurog1* and *utNgn1* in the neocortex were dramatically reduced during development (Figs. S2*C* and S6). We then examined whether the suppression of *utNgn1* production in the late stage of development is mediated by PcG proteins. To this end, we induced the conditional ablation of Ring1B, an essential component of Polycomb repressive complex 1 (37), by injecting tamoxifen intraperitoneally into *Ring1b*$^{flox/flox}$; NestinERT2-Cre mice (18, 38) at E12.5. The amount of *utNgn1* was markedly greater in the neocortex isolated from the Ring1B-deficient embryos at E18.5 compared with control embryos (Fig. 5*D*). Together, these results indicate that PcG proteins suppress *utNgn1* expression during the late stage of neocortical NPC development. PcG proteins thus appear to regulate *Neurog1* expression not simply by direct suppression of the gene itself but also by that of its enhancer.

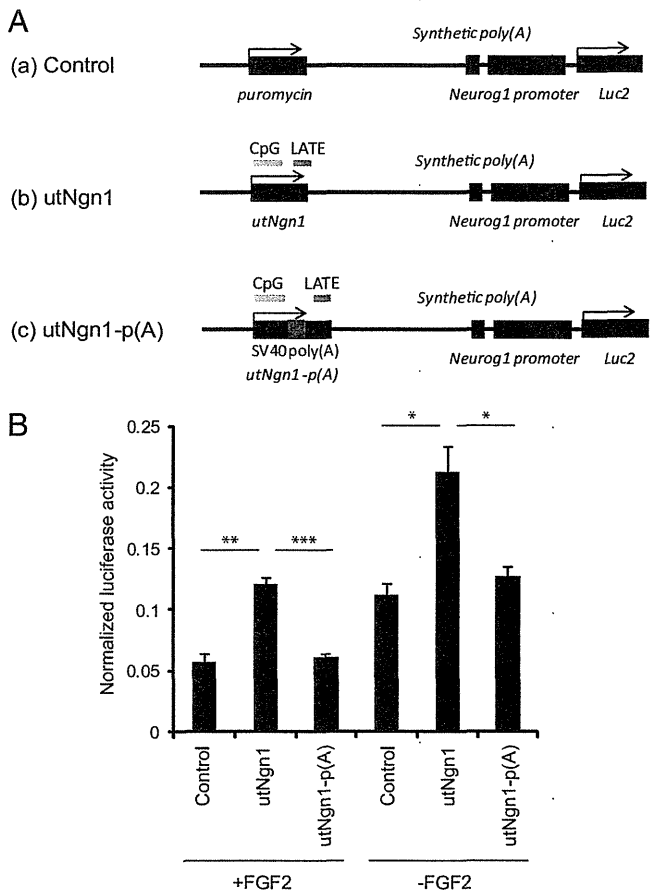

Fig. 4. Full-length *utNgn1*, but not truncated *utNgn1*, promotes expression of reporter gene. (*A*) Schematic representation of the reporter constructs. A 2.7-kb region of the Neurog1 promoter was cloned into the promoter multicloning site of the pGL4.20 vector and used as a control (*a*). Full-length *utNgn1* was cloned and inserted into the upstream region of vector *a* (*b*). Two SV40 poly(A) sequences were tandemly inserted into the *utNgn1* region between the CGI and the LATE enhancer (*c*). (*B*) Luciferase reporter assay. Firefly vectors shown in *A* and the control Renilla vector were transfected into NPCs prepared from E11.5 neocortices. All cells were cultured with FGF2 for 12 h and then half were cultured with and half without FGF2 for 20 h. Data are normalized by the Renilla luciferase activity and are means ± SEM ($n = 3$). $*P < 0.05$, $**P < 0.01$, $***P < 0.001$ by two-tailed Student *t* test.

Discussion

A significant portion of the mammalian genome generates noncoding RNAs (ncRNAs) including long intervening noncoding RNAs (lincRNAs) (39–41), some of which have been implicated in gene silencing associated with processes such as imprinting and X chromosome inactivation (42). However, recent studies have also begun to reveal roles of lincRNAs in gene activation (23–25). For instance, a set of ncRNAs (ncRNA-a) was shown to positively regulate their neighboring protein-coding genes, including those for *SCL*, *Snail1*, and *Snail2* (24). Similarly, *HOTTIP*, a lincRNA transcribed from the 5′ end of the *HoxA* locus, was found to positively regulate the *HoxA* gene cluster (23). Our results now indicate that *utNgn1* is another lincRNA that positively regulates gene expression.

Recent genome-wide studies have revealed that gene promoters are marked by H3K4me3, whereas enhancers are often associated with H3K4me1 but are devoid of H3K4me3 (43). The enhancer region now shown to encode *utNgn1* therefore appears to be atypical in that it is associated with H3K4me3. Because this is also the case for the ncRNA-a and *HOTTIP* loci, the presence of H3K4me3 in the enhancer regions might be a specific characteristic of regions encoding this "gene activator" class of lincRNAs. H3K4me1-enriched enhancers have also been shown to express RNA (eRNA), although the functions of these RNA molecules are unknown (21, 26). The transcripts from H3K4me1-enriched enhancers are devoid of polyadenylation, whereas long noncoding RNAs transcribed from H3K4me3-enriched enhancers including *utNgn1* harbor polyadenylation, possibly reflecting a difference in mode of regulation and/or function (21, 23–26). *utNgn1* is more similar to lincRNAs in this context, although the *utNgn1* locus does not harbor the H3K36me3 mark, which is a characteristic of lincRNAs.

Development is associated with strict regulation of the enhancers of developmental genes. It has been proposed that H3K4me1-enriched enhancers can be classified as either "poised" and "active" enhancers by the additional presence of the histone marks H3K27me3 and H3K27ac, respectively (44, 45). It remains unclear, however, whether these histone marks are functionally important for enhancer activity. Our results now suggest that the

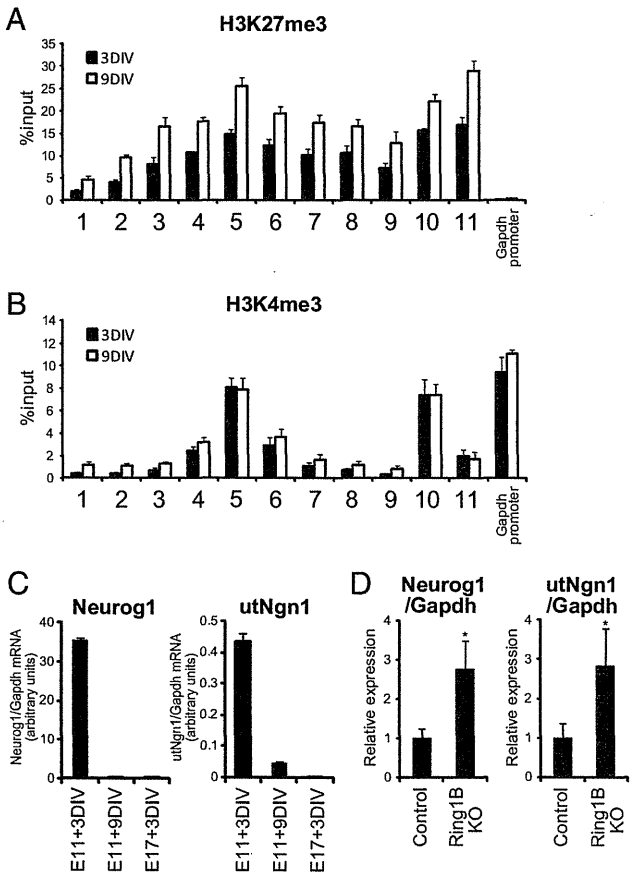

Fig. 5. PcG proteins repress the expression of *utNgn1* in the late stage of NPC development. (*A* and *B*) Primary NPCs isolated from the E11.5 neocortex were cultured for 3 or 9 DIV in suspension in the presence of FGF2 and EGF. Cells were then subjected to ChIP assays with antibodies to H3K27me3 (*A*) or to H3K4me3 (*B*) and with the PCR primers indicated in Fig. 1*A*. Data are means ± SEM from three independent experiments. (*C*) Primary NPCs isolated from the E11.5 or E17.5 neocortex were cultured for 3 or 9 DIV as in *A*, after which total RNA was isolated and subjected to qRT-PCR analysis of *utNgn1* and *Neurog1* mRNA. Data are normalized by the amount of *Gapdh* mRNA and are means ± SEM ($n = 3$). (*D*) Total RNA prepared from the neocortex of E18.5 *Ring1b*$^{flox/flox}$; NestinERT2-Cre (Ring1B KO) and *Ring1-b*$^{flox/flox}$ (control) embryos that were exposed to tamoxifen in utero at E12.5 were subjected to qRT-PCR analysis of *Neurog1* mRNA and *utNgn1*. Data are normalized by the amount of *Gapdh* mRNA, are expressed relative to the corresponding value for control embryos, and are means ± SD from three embryos of each genotype. $*P < 0.05$ (Student *t* test).

utNgn1 locus is maintained in a poised (or inactive) state in the late stage of neocortical NPC development by a PcG protein-mediated mechanism, given that the locus is enriched with both H3K27me3 and H3K4me3 and that *utNgn1* expression was derepressed by ablation of Ring1B. These findings thus suggest that PcG proteins may directly suppress enhancers in addition to promoters for a class of developmental genes in a developmental context-dependent manner.

The mechanism of enhancers' regulation of gene expression and that of the regulation of enhancers themselves are fundamental to an understanding of gene control mechanisms. Given our finding that *utNgn1* is necessary for the efficient activation of *Neurog1* expression, a next key question will be how this transcript promotes gene activation, which is likely by recruitment of effector proteins, including histone modifiers or transcription factors, to the *Neurog1* promoter. Although recruitment or maintenance of mixed lineage leukemia (MLL) complex is implicated in the action of lincRNAs such as *HOTTIP* and *Mistral* (23, 25), other mechanisms likely account for the action of *utNgn1*, because the level of H3K4me3 (mediated by MLL complex) of the *Neurog1* promoter was not significantly reduced, despite a marked reduction of *utNgn1* expression, in the late developmental stages (Fig. 5). It will also be important to elucidate how PcG protein-mediated regulation of the *utNgn1* locus relates to that of the *Neurog1* promoter. It is possible that PcG proteins associated with the enhancer might physically and functionally interact with those associated with the promoter. Further elucidation of *utNgn1*'s regulation and function should bring new insights into the role of enhancers and the regulation of transcription.

Materials and Methods

Full details of procedures are provided in *SI Materials and Methods*. Briefly, primary NPCs were isolated and cultured as described previously (18). The siRNA were transfected using Neon transfection system (Invitrogen). Antibodies used in ChIP assay were anti-H3K9K14Ac (Upstate; 06–599), anti-H3K27me3 (Upstate; 07–449), anti-H3K4me3 (Active Motif; 39916), anti-H3K36me3 (Abcam; 9050), and control rabbit IgG (Santa Cruz; sc-2027).

ACKNOWLEDGMENTS. We thank Drs. Yoshiki Sasai, Mototsugu Eiraku, and Tokushige Nakano for instruction, materials, and cell lines on ES cell culture and NPC induction; and Dr. Ryoichiro Kageyama for Nes-CreERT2 mice; and Dr. Yukihide Tomari, Kei Akaiwa, and Taruho Endoh for technical assistance. This work was supported by Core Research for Evolutional Science and Technology (CREST) of the Japan Science and Technology Agency, Grant-in-Aid for Scientific Research on Innovative Areas "Neural Diversity and Neocortical Organization" and "Cell Fate" from the Ministry of Education, Culture, Sports, Science and Technology (MEXT) of Japan, by Grant-in-Aid for Scientific Research (A) from MEXT of Japan, by Grant-in-Aid for JSPS fellows from JSPS, and by the Global COE Program (Integrative Life Science Based on the Study of Biosignaling Mechanisms), MEXT, Japan. M.O. is a research fellow of the Japan Society for the Promotion of Science (JSPS).

1. Hirabayashi Y, Gotoh Y (2010) Epigenetic control of neural precursor cell fate during development. *Nat Rev Neurosci* 11:377–388.
2. Miller FD, Gauthier AS (2007) Timing is everything: Making neurons versus glia in the developing cortex. *Neuron* 54:357–369.
3. Guillemot F (2007) Cell fate specification in the mammalian telencephalon. *Prog Neurobiol* 83:37–52.
4. Ma QF, Kintner C, Anderson DJ (1996) Identification of neurogenin, a vertebrate neuronal determination gene. *Cell* 87:43–52.
5. Fode C, et al. (2000) A role for neural determination genes in specifying the dorsoventral identity of telencephalic neurons. *Genes Dev* 14:67–80.
6. Gowan K, et al. (2001) Crossinhibitory activities of Ngn1 and Math1 allow specification of distinct dorsal interneurons. *Neuron* 31:219–232.
7. Cau E, Casarosa S, Guillemot F (2002) Mash1 and Ngn1 control distinct steps of determination and differentiation in the olfactory sensory neuron lineage. *Development* 129: 1871–1880.
8. Schuurmans C, et al. (2004) Sequential phases of cortical specification involve Neurogenin-dependent and -independent pathways. *EMBO J* 23:2892–2902.
9. Sun Y, et al. (2001) Neurogenin promotes neurogenesis and inhibits glial differentiation by independent mechanisms. *Cell* 104:365–376.
10. Cai L, Morrow EM, Cepko CL (2000) Misexpression of basic helix-loop-helix genes in the murine cerebral cortex affects cell fate choices and neuronal survival. *Development* 127: 3021–3030.
11. Blader P, Plessy C, Strähle U (2003) Multiple regulatory elements with spatially and temporally distinct activities control neurogenin1 expression in primary neurons of the zebrafish embryo. *Mech Dev* 120:211–218.
12. Blader P, et al. (2004) Conserved and acquired features of neurogenin1 regulation. *Development* 131:5627–5637.
13. Nakada Y, Parab P, Simmons A, Omer-Abdalla A, Johnson JE (2004) Separable enhancer sequences regulate the expression of the neural bHLH transcription factor neurogenin 1. *Dev Biol* 271:479–487.
14. Quiñones HI, Savage TK, Battiste J, Johnson JE (2010) Neurogenin 1 (Neurog1) expression in the ventral neural tube is mediated by a distinct enhancer and preferentially marks ventral interneuron lineages. *Dev Biol* 340:283–292.
15. Hirabayashi Y, et al. (2004) The Wnt/beta-catenin pathway directs neuronal differentiation of cortical neural precursor cells. *Development* 131:2791–2801.
16. Israsena N, Hu M, Fu WM, Kan LX, Kessler JA (2004) The presence of FGF2 signaling determines whether beta-catenin exerts effects on proliferation or neuronal differentiation of neural stem cells. *Dev Biol* 268:220–231.
17. Holm PC, et al. (2007) Loss- and gain-of-function analyses reveal targets of Pax6 in the developing mouse telencephalon. *Mol Cell Neurosci* 34:99–119.
18. Hirabayashi Y, et al. (2009) Polycomb limits the neurogenic competence of neural precursor cells to promote astrogenic fate transition. *Neuron* 63:600–613.
19. Ong CT, Corces VG (2011) Enhancer function: New insights into the regulation of tissue-specific gene expression. *Nat Rev Genet* 12:283–293.
20. Blackwood EM, Kadonaga JT (1998) Going the distance: A current view of enhancer action. *Science* 281:60–63.
21. Kim TK, et al. (2010) Widespread transcription at neuronal activity-regulated enhancers. *Nature* 465:182–187.
22. De Santa F, et al. (2010) A large fraction of extragenic RNA pol II transcription sites overlap enhancers. *PLoS Biol* 8:e1000384.
23. Wang KC, et al. (2011) A long noncoding RNA maintains active chromatin to coordinate homeotic gene expression. *Nature* 472:120–124.
24. Ørom UA, et al. (2010) Long noncoding RNAs with enhancer-like function in human cells. *Cell* 143:46–58.
25. Bertani S, Sauer S, Bolotin E, Sauer F (2011) The noncoding RNA Mistral activates Hoxa6 and Hoxa7 expression and stem cell differentiation by recruiting MLL1 to chromatin. *Mol Cell* 43:1040–1046.
26. Wang D, et al. (2011) Reprogramming transcription by distinct classes of enhancers functionally defined by eRNA. *Nature* 474:390–394.
27. Zhou VW, Goren A, Bernstein BE (2011) Charting histone modifications and the functional organization of mammalian genomes. *Nat Rev Genet* 12:7–18.
28. Deaton AM, Bird A (2011) CpG islands and the regulation of transcription. *Genes Dev* 25:1010–1022.
29. Sandelin A, et al. (2007) Mammalian RNA polymerase II core promoters: insights from genome-wide studies. *Nat Rev Genet* 8:424–436.
30. Chen LL, Carmichael GG (2010) Decoding the function of nuclear long non-coding RNAs. *Curr Opin Cell Biol* 22:357–364.
31. Mercer TR, Dinger ME, Mattick JS (2009) Long non-coding RNAs: Insights into functions. *Nat Rev Genet* 10:155–159.
32. Maric D, Fiorio Pla A, Chang YH, Barker JL (2007) Self-renewing and differentiating properties of cortical neural stem cells are selectively regulated by basic fibroblast growth factor (FGF) signaling via specific FGF receptors. *J Neurosci* 27: 1836–1852.
33. Gaiano N, Fishell G (2002) The role of notch in promoting glial and neural stem cell fates. *Annu Rev Neurosci* 25:471–490.
34. Eiraku M, et al. (2008) Self-organized formation of polarized cortical tissues from ESCs and its active manipulation by extrinsic signals. *Cell Stem Cell* 3:519–532.
35. Ebisuya M, Yamamoto T, Nakajima M, Nishida E (2008) Ripples from neighbouring transcription. *Nat Cell Biol* 10:1106–1113.
36. Bernstein BE, et al. (2006) A bivalent chromatin structure marks key developmental genes in embryonic stem cells. *Cell* 125:315–326.
37. Simon JA, Kingston RE (2009) Mechanisms of polycomb gene silencing: Knowns and unknowns. *Nat Rev Mol Cell Biol* 10:697–708.
38. Calés C, et al. (2008) Inactivation of the polycomb group protein Ring1B unveils an antiproliferative role in hematopoietic cell expansion and cooperation with tumorigenesis associated with Ink4a deletion. *Mol Cell Biol* 28:1018–1028.
39. Carninci P, et al.; FANTOM Consortium; RIKEN Genome Exploration Research Group and Genome Science Group (Genome Network Project Core Group) (2005) The transcriptional landscape of the mammalian genome. *Science* 309:1559–1563.
40. Guttman M, et al. (2009) Chromatin signature reveals over a thousand highly conserved large non-coding RNAs in mammals. *Nature* 458:223–227.
41. Khalil AM, et al. (2009) Many human large intergenic noncoding RNAs associate with chromatin-modifying complexes and affect gene expression. *Proc Natl Acad Sci USA* 106: 11667–11672.
42. Ponting CP, Oliver PL, Reik W (2009) Evolution and functions of long noncoding RNAs. *Cell* 136:629–641.
43. Heintzman ND, et al. (2007) Distinct and predictive chromatin signatures of transcriptional promoters and enhancers in the human genome. *Nat Genet* 39: 311–318.
44. Rada-Iglesias A, et al. (2011) A unique chromatin signature uncovers early developmental enhancers in humans. *Nature* 470:279–283.
45. Creyghton MP, et al. (2010) Histone H3K27ac separates active from poised enhancers and predicts developmental state. *Proc Natl Acad Sci USA* 107:21931–21936.